Tbx1 ortholog *org-1* is required to establish testis stem cell niche identity in *Drosophila*

Patrick Hofe[1], Tynan Gardner[2], Stephen DiNardo[2], Lauren Anllo[1]*

[1] Department of Biology, East Carolina University, Greenville, NC 27858

[2] Perelman School of Medicine at the University of Pennsylvania, Philadelphia, PA 19104

*Communicating author: anllol22@ecu.edu

Abstract:

Stem cells require signals from a cellular microenvironment known as the niche that regulates identity, location, and division of stem cells. Niche cell identity must be properly specified during development to form a tissue capable of functioning in the adult. Here, we show that the Tbx1 ortholog *org1* is expressed in *Drosophila* testis niche cells in response to Slit and FGF signals. *org1* is expressed during niche development and is required to specify niche cell identity. *org1* mutants specified fewer niche cells, and those cells showed disruption of niche-specific markers, including loss of the niche adhesion protein Fas3 and reduced *hedgehog* expression. We found that *org1* expression in somatic gonadal precursors is capable of inducing formation of additional niche cells. Disrupted niche identity in *org1* mutants resulted in niche assembly and functionality defects. We find the conserved transcription factor *islet* is expressed in response to *org1* and show that *islet* functions downstream to mediate niche identity and assembly. This work identifies a novel role for *org1* in niche establishment.

Summary Statement:

Specification of niche identity is crucial to establish a functional stem cell microenvironment. Using a translatable model, we show that niche expression of *org1* influences *islet* to specify niche identity.

20 **Introduction:**

21 Stem cells play a vital role in maintaining functional tissues and organs. The
22 preservation of stem cells in many tissues is controlled by the stem cell niche, a local cellular
23 microenvironment that supplies signals to maintain stem cell identity, location, and division rates
24 (Li & Xie, 2005). A key concept in stem cell niche biology is the use of diffusible signals to
25 regulate stem cell behaviors. In models like the mammalian intestinal stem cell (ISC) niche,
26 diffusible signals such as Wnt, Hh, and BMP ligands have been shown to regulate stem cells
27 (Walker et al., 2008). These signals have varying origins since there are multiple cell types that
28 comprise the intestinal stem cell niche (Walker et al., 2008). Because various cell lineages can
29 comprise the niche, the identification of niche cells is often challenging. In some tissues even
30 the identity of the stem cells is unclear (Sato et al., 2011; Kaestner, 2019; Li et al., 2023). Thus,
31 identifying regulators that specify niche identity during tissue development has remained a
32 challenge in stem cell biology.

33 Because of its readily identifiable and well-defined niche, we leverage the *Drosophila*
34 testis to study how niche cells acquire their identity and adopt proper function during
35 development (de Cuevas & Matunis, 2011; Le Bras & Van Doren, 2006; Anllo et al., 2019;
36 Okegbe & DiNardo, 2011; Wingert & DiNardo, 2015). The *Drosophila* testis is a paradigmatic
37 niche in which many concepts at the foundation of stem cell biology continue to be elucidated
38 (Herrera & Bach, 2019; Leatherman & DiNardo 2008 and 2010; Lenhart & DiNardo 2015; Inaba
39 et al., 2015; Tulina & Matunis 2001; Yamashita et al., 2003; Zheng et. al., 2011). The singular
40 cell type that makes up the *Drosophila* testis niche, somatic “hub” cells, regulates both germline
41 and somatic stem cells required to maintain sperm production throughout the adult life of the fly
42 (Lenhart and DiNardo, 2015; Roach and Lenhart, 2024). The wealth of powerful genetic tools
43 available to study this niche make it an ideal model to identify regulators of niche cell fate.

44 Prior to niche formation, the embryonic Stage 15 *Drosophila* testis consists of a spherical
45 arrangement of somatic gonadal precursors (SGPs) interspersed among and encysting germ

46 cells (Jenkins et al., 2003; Le Bras & Van Doren, 2006). SGPs are specified from a subset of
47 mesodermal cells adjacent to muscle precursors in embryonic parasegments 10-13 earlier in
48 embryogenesis (Boyle et al., 1995; Boyle et al., 1997; Riechmann et al., 1998). Niche, or "hub,"
49 cells derive from SGPs, and are specified through Notch signaling (Kitadate & Kobayashi, 2010;
50 Okegbe & DiNardo, 2011; DiNardo et al., 2011). By stage 11 of embryogenesis, SGPs
51 contacting the primordial midgut receive Delta ligands which initiate Notch signaling and niche
52 specification (Okegbe & DiNardo, 2011). Later, SGPs at the gonad anterior receive the Notch
53 ligand Serrate from other gonadal cells, and SGPs at the posterior receive EGFR antagonistic
54 signals that repress niche identity (Kitadate & Kobayashi, 2010). Defects in Notch signaling
55 result in fewer niche cells specified (Okegbe & DiNardo, 2011; DiNardo et al., 2011; Kitadate &
56 Kobayashi, 2010; Wingert & DiNardo, 2015). Specified niche cells downregulate the conserved
57 Maf transcription factor Traffic jam (Tj) in response to Notch signaling (Winger & DiNardo,
58 2015). A role for Notch signaling in niche formation has translated to other niches in *Drosophila*
59 and in mammals (Zamfirescu et al., 2022). Outside of Notch signaling, there is little known about
60 how testis niche cells acquire their identity.
61 Once specified, embryonic niche cells are compartmentalized to the gonad anterior in a
62 process called niche assembly (Le Bras and Van Doren, 2006; Anllo et al., 2019). During
63 assembly, specified prospective (pro) niche SGPs move peripherally onto the gonadal
64 extracellular matrix (ECM), where they then migrate to their anterior assembly position (Anllo et
65 al., 2019). Our previous work revealed that extrinsic Slit and FGF signals from neighboring
66 visceral muscle (Vm) are required for this migration (Anllo & DiNardo, 2022). At the gonad
67 anterior, niche cells first exhibit F-actin polarization to niche-niche interfaces, which later re-
68 polarizes to niche-stem cell interfaces as niche cells compact into a spherical arrangement with
69 smooth contour (Anllo & DiNardo, 2022; Warder et al., 2024). Germline stem cells contacting
70 the assembled niche contribute to niche morphogenesis through actomyosin networks that
71 result in tension around the compacting hub periphery (Warder et al., 2024). The assembled

72 and compacted niche expresses niche specific markers such as *fasciclin* 3 and *hedgehog* and is
73 radially surrounded by germline stem cells (GSCs) and later, cyst stem cells (CySCs) (Le Bras
74 & Van Doren, 2006; Sheng et al., 2009; Sinden et al., 2012; Wingert & DiNardo, 2015). The
75 niche makes adhesive connection to neighboring stem cells and extracellular matrix to maintain
76 its shape, location, and function (Lee et al., 2008; Vida et al., 2024; Tanentzapf et al., 2007;
77 Tseng et al., 2022; Amoyel et al., 2013).

78 After niche establishment, the niche functions throughout the life of the animal. The
79 niche's location, critical to maintain GSCs and CySCs, is maintained through Integrin-mediated
80 connections to the ECM (Anllo et al. 2019; Lee et al., 2008; Tanentzapf et al., 2007). In its
81 established position, the niche sends maintenance signals to its surrounding stem cells,
82 including Unpaired (Upd) and Hedgehog (Hh). Upd ligands activate JAK/STAT signaling in
83 GSCs, which regulates their adhesion to the niche and oriented cell divisions (Chen et. al.,
84 2018; Leatherman & DiNardo 2008 and 2010; Tulina & Matunis, 2001; Wawersik et al., 2005;
85 Yamashita et al., 2003). Niche-secreted Hedgehog regulates CySC self-renewal (Amoyel et al.,
86 2012). Niche signals are important for establishing the stem cell populations, and for long term
87 stem cell maintenance (Sheng et al., 2009; Sinden et al., 2012).

88 Because Notch signaling required to specify niche cells is initiated at stage 11 of
89 embryogenesis (Okegbe & DiNardo, 2011), and niche-specific markers such as Fas3
90 accumulation are not observed until stage 15 of embryogenesis (Le Bras & Van Doren, 2006;
91 Anllo et al., 2019), there are likely other factors influencing the specification of niche cells during
92 this period. Our work here identifies the Tbx1 ortholog *org1* as one of those factors. Tbx1 and its
93 orthologs play a conserved role across phyla in specifying mesodermal cell types (Marcellini et
94 al., 2003). Like Tbx1*, org1* encodes a transcription factor with a T-box DNA binding domain and
95 is a known regulator of mesodermal muscle fate during embryonic development (Schaub et al.
96 2012; Schaub & Frasch, 2013; Boukhatmi et al., 2014). Our previous work identified that the
97 conserved transcription factor *islet* is expressed in niche cells and required for both niche

assembly and cytoskeletal polarization downstream of Vm assembly cues (Anllo & DiNardo, 2022). *islet* expression is known to be regulated by *org1* during specification of alary musculature (Boukhatmi et al., 2014). Here, we find that a parallel mechanism regulates specification of niche cells and directs their anterior assembly. We show that *org1* is expressed in the embryonic niche and reveal its requirement in establishing a full complement of functional, assembled niche cells. We further show that Org1 accumulation depends on Slit and FGF signals, and that *islet* acts downstream of *org1*. These data reveal *org1* as a novel regulator of niche identity and assembly for the *Drosophila* testis niche.

107 **Results:**

108 ***org1* is expressed in the niche and is induced by signals from visceral muscle.**

109 Our previous work has shown that the conserved transcription factor *islet* is expressed in the
110 developing niche (Anllo & DiNardo, 2022). Because Org1 is a known regulator of *islet*
111 expression in other tissues (Boukhatmi et al., 2014), and because single nuclear RNA sequence
112 data (snRNAseq) suggested that *org1* is highly enriched in the adult testis niche (Li et al., 2021;
113 Raz et al. 2023), we tested whether *org1* was expressed in the developing gonadal niche. We
114 observed expression of an Org1::GFP transgenic reporter (Kudron et al., 2018) in prospective
115 niche cells beginning prior to assembly at embryonic stage 15/16 and after niche assembly in
116 stage 17 at the gonad anterior (Figure 1A-1C'). *org1* expression in some prospective niche cells
117 coincided with the timing of Traffic jam downregulation (Figure 1A', 1B'). Additionally, we also
118 saw SGPs without downregulated Traffic jam that exhibited lower expression of *org1* elsewhere
119 in the gonad (Figure 1B-B", yellow arrows). We confirmed the stage 17 *org1* expression pattern
120 using an Org1 antibody (Schaub et al., 2012) that revealed a signal in gonadal niche cell nuclei
121 (Figure 1B, B') which was absent in *org1* mutants (Figure S1). Our findings reveal that *org1* is
122 expressed in the gonad niche, and its expression begins before niche assembly.

123

124 Since *islet* is regulated by Slit and FGF signals from the visceral muscle (Vm), we tested if *org1*
125 is also regulated by these signals (Anllo and DiNardo, 2022). If *org1* is induced by these signals,
126 then loss of Slit and FGF Vm signals required for niche assembly would result in loss of Org1
127 accumulation in niche cells. Indeed, loss of both signals together resulted in diminished Org1
128 accumulation (Figure 1E-1F'). Additionally, loss of either Slit or FGF separately resulted in
129 diminished Org1 accumulation (Figure 1G-1H') and our fluorescence quantifications supported
130 these findings (Figure 1I-1K). Together, our data confirm that *org1* is expressed in the niche and
131 accumulates in response to Slit and FGF.

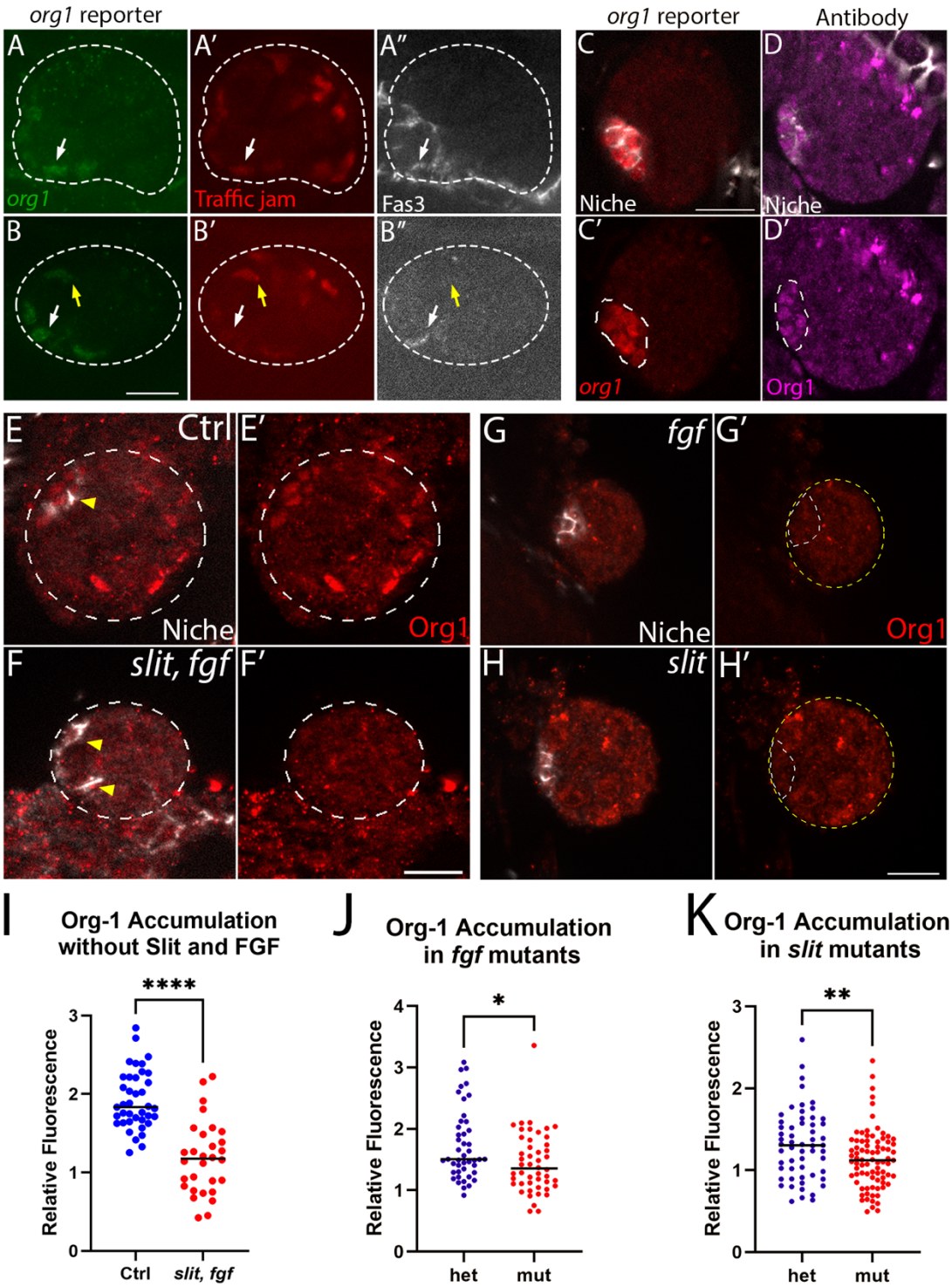

Figure 1. *org1* is expressed in the niche in response to visceral muscle signals. (A-B') Gonads (dotted line) from Stage 15 animals with the Org1::GFP reporter, immunostained for GFP (green) and Traffic jam (red). Fas3 (white) accumulates at assembling niche cell interfaces. Org1::GFP is brightest when Traffic jam (red) is downregulated. Prospective niche cells with downregulated Traffic jam (white arrows) and with Traffic jam not downregulated

138 (yellow arrows). (C, C') Org1::GFP reporter (red) showed *org1* expression in the assembled
139 niche (dotted white line; Fas3, white). (D, D') Org1 antibody (magenta) revealed accumulation in
140 the niche (dotted white line; Fas3, white) with spurious non-specific signal at the posterior (see
141 Suppl Fig S1). (E, E') Control gonads showed Org1 (red) accumulation in the niche (white). (F,
142 F') *slit, fgf* mutants had diminished accumulation of Org1. Gonads are outlined with dotted white
143 lines. (G-G') *fgf* mutants have diminished Org1 accumulation in the niche. (H, H') *slit* mutants
144 had diminished Org1 accumulation in the niche. Gonads are outlined in yellow; niches are
145 outlined in white. (I) Quantification of Org-1 accumulation in niche cells in controls and visceral
146 muscle signaling mutants ($p<0.0001$, Ctrl n=39 niche cells from 13 gonads; *slit, fgf* n= 30 niche
147 cells, from 10 gonads Mann-Whitney Test). (J) Quantification of Org1 accumulation in *fgf*
148 mutants and heterozygous sibling controls (Het) ($p= 0.0136$, Het n=45 niche cells from 15
149 gonads; *fgf* n=48 niche cells from 16 gonads, Mann-Whitney Test). (K) Quantification of Org1
150 accumulation in *slit* mutants and heterozygous sibling controls (Het) ($p= 0.0090$, Het n=57 niche
151 cells from 19 gonads; *slit* n=81 niche cells from 27 gonads, Mann-Whitney Test). All
152 quantifications are shown for individual niche nuclei. Scale bars, 10um.
153

154 ***org1* is necessary and sufficient to induce niche cell fate.**

155 Given the known role of *org1* in embryonic muscle specification, we asked if there were niche
156 identity defects in *org1* mutants (Schaub & Frasch, 2012; Boukhatmi et al., 2014). We
157 hypothesized that if *org1* had a role in specifying niche cell fate, we would see disruption of
158 niche identity markers. We assayed for niche identity markers Fasciclin3 (Fas3) accumulation
159 and *hedgehog* (*hh*) expression (Le Bras & Van Doren, 2006; Wingert & DiNardo, 2015) in an
160 *org1* mutant allele lacking the translation initiation codon and T-box domain (Schaub et al.,
161 2012). *org1* mutants did not accumulate the niche specific adhesion protein Fasciclin 3 (Figure
162 2B-2B'). Additionally, *org1* mutants had lower expression of a *hh*-lacZ reporter in niche cells
163 compared to controls (Figure 2C-2E). Interestingly, *hh* expression is known to be restricted to
164 the adult niche (Amoyel et. al., 2013). We find that while *hh* expression is highest in control
165 embryonic niche cells, we do detect low levels of *hh* in some control SGPs outside the niche
166 (Figure S2). Since these niche identity markers were disrupted, we used N-cadherin (N-cad)
167 accumulation to detect niche cells in *org1* mutants. N-cad accumulation is enriched in the cortex
168 of properly assembled niche cells at the gonad anterior, with low accumulation in other SGPs,
169 affording a reasonable measure of identification of niche cells at the anterior (Le Bras & Van

170 Doren, 2006). When visualizing gonads with N-cad immunofluorescence, we detected fewer N-
171 cad accumulating niche cells in *org1* mutants compared to controls (Figure 2F-2G').
172
173 To confirm that the fewer N-cad accumulating niche cells in *org1* mutants resulted from failure to
174 specify niche cells and not simply a reduction in the number of SGPs, we quantified the total
175 number of SGPs in *org1* mutants. We assayed the SGP-specific transcription factor Traffic jam
176 (Tj) to count all SGPs (Wingert & DiNardo, 2015). While there was a slight decrease in number of
177 SGPs, the fraction of these cells specified into niche cells was significantly lower in *org1* mutants
178 compared to control gonads (Figure S3). Together with our data indicating a loss of the niche
179 specific adhesion protein Fas3 and reduction of *hh* gene expression in the niche, these results
180 support a role for *org1* in niche specification (Figure 2, S3). Interestingly, *org1* mutant niche cells
181 still down regulated *tj* as in normal niches, indicating that some aspects of niche specification
182 occur (Figure S3).
183
184 Since *org1* mutants had fewer niche cells, we tested whether overexpression of *org1* in all
185 SGPs would create more niche cells. Indeed, when we overexpressed *org1* with a somatic
186 lineage-specific driver (*six4*-gal4; Anllo et. al., 2019), we generated additional N-cad
187 accumulating niche cells at the gonad anterior (Figure 2I-K). Together, our data suggest that
188 *org1* plays a role in specifying niche identity and is sufficient to induce niche identity in additional
189 SGPs.

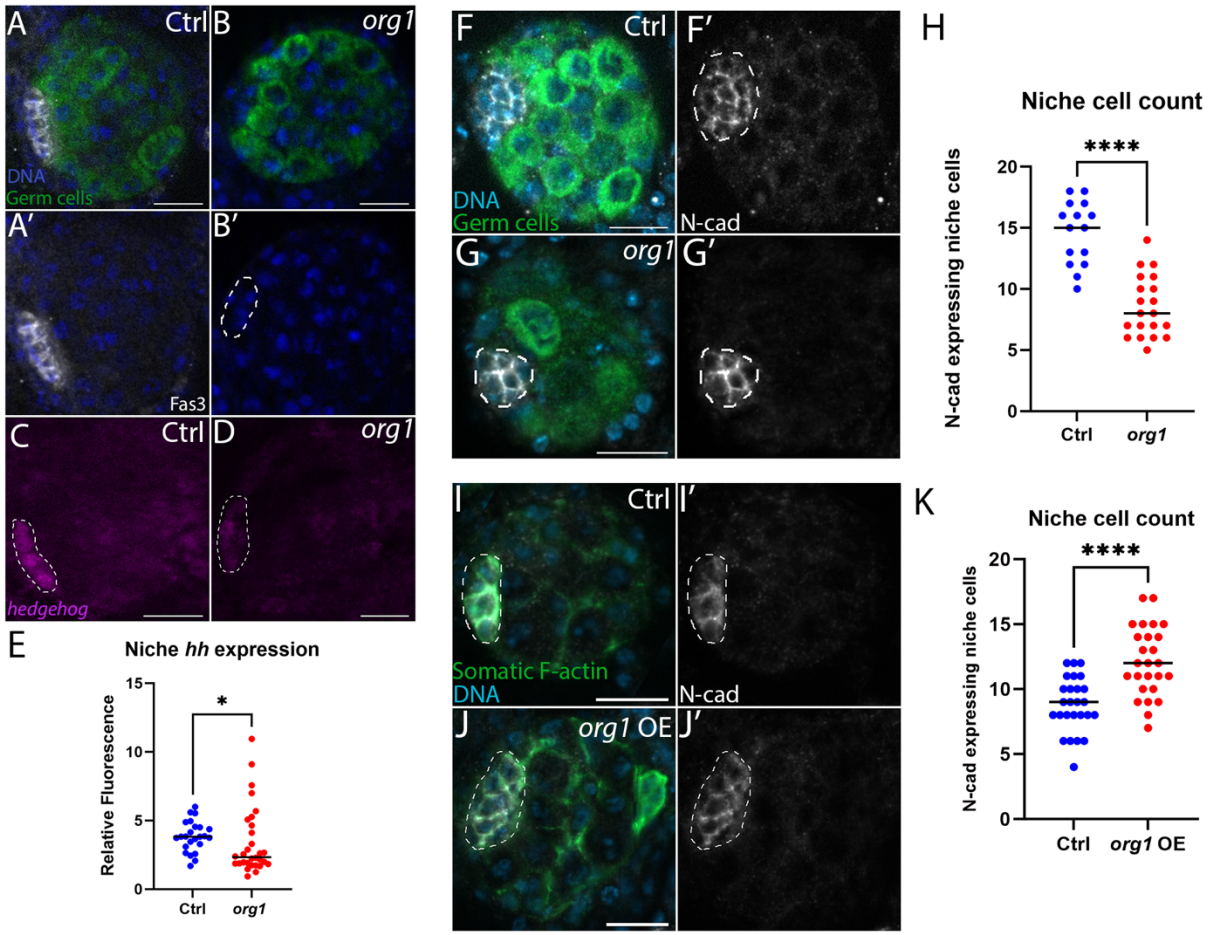

Figure 2. *org1* is necessary and sufficient to induce niche cell fate. (A-D) Dissected gonads immunostained to show germ cells (green), Fas3 (white), *hh*-lacZ (magenta), DNA (blue). (A, A', C) Control niche cells accumulated niche specific markers Fas3 and *hedgehog* reporter expression (*hh*-lacZ, separate gonad from A, A'). (B, B', D) *org1* mutants did not accumulate Fas3 and had diminished expression of *hh*-lacZ reporter (D is a separate gonad from B). (E) Quantification of *hh*-lacZ expression in niche cells accumulating N-cad ($p= 0.0294$, Ctrl n=24 niche cells from 7 gonads; *org1* n=30 niche cells from 10 gonads, Mann-Whitney Test). (F, F') Control gonads accumulated enriched N-cad at the cortex of niche cells. (G, G') *org1* mutant niches had fewer cells accumulating enriched N-cad. (F-G') Germ cells (green), N-cad (white), DNA (blue). (H) Quantification of N-cad accumulating niche cells per gonad ($p<0.0001$, Ctrl n=15 gonads; *org1* n=20 gonads, Mann-Whitney Test). (I, I') Control gonad with *six4*moesinGFP marking somatic F-actin. (J, J') SGP driven *org1* overexpression in gonads generated niches that had more cells in comparison to controls. (I-J') Somatic cells (green), Niche (white), DNA (blue). (K) Quantification of niche cell count ($p<0.0001$, Ctrl n=26 gonads; *org1* n=26 gonads, Mann-Whitney Test). Dotted lines, niche. Scale bars, 10 um.

***org1* is required SGP intrinsically for niche identity and assembly.**

The data above were collected from a whole organism *org1* mutant line in which all T-box binding domains were excised (Schaub et al., 2012). To test whether *org1* is necessary in SGPs for niche cell identity we manipulated *org1* expression in the SGP lineage. We used two somatic

211 lineage-specific drivers that varied in strength, *six4*VP16-gal4 (Warder et al., 2024) and *six4*-
212 gal4 to knock down *org1* expression. Using the weaker driver (*six4*-gal4), we found an expected
213 decrease in niche cell number, and Fas3 accumulation appeared reduced (Figure S4).
214 Assuming this driver generates only a partial knockdown, this suggests a stringent requirement
215 of *org1* in niche cell specification (See Discussion). Excitingly, using the stronger driver
216 (*six4*VP16-gal4), we saw both fewer niche cells (Figure 3A-3C), and dispersed niche cells
217 accumulating low levels of Fas3 (Figure 3B'-3B'', 3D). It is possible this dispersed phenotype
218 was not something we could observe in the global *org1* mutants due to the complete loss of
219 Fas3 (Figure 2). Other niche cells markers, including E-cad and N-cad, accumulate on control
220 non-niche SGPs to a degree, so dispersed niche cells might not have been apparent (Figure
221 S5). Our data suggest that *org1* is primarily a specification factor during niche establishment
222 and secondarily affects niche assembly.

223 To further support an SGP intrinsic requirement for *org1* during niche establishment, we
224 performed a tissue-specific rescue experiment. We expressed *org1* with our somatic lineage
225 specific driver, *six4*-gal4, in whole organism *org1* mutants and observed rescued Fas3
226 accumulation (Figure 3E-3H'). Our rescue experiment simultaneously expressed the F-actin
227 label Ftractin-tdTomato in SGPs which allowed us to analyze cytoskeletal polarity of niche cells.
228 Our previous work has shown that F-actin polarizes to niche-stem cell interfaces after assembly
229 is complete (Anllo & DiNardo, 2022; Warder et al., 2024). We noted that while polarization of F-
230 actin at niche-stem cell interfaces is disrupted in *org1* mutant niche cells, this polarization was
231 rescued with *org1* overexpression in SGPs (Fig 3F-K, see arrows). These data suggest that
232 *org1* in SGPs is sufficient to initiate downstream cell biological events that polarize F-actin in the
233 assembled niche.

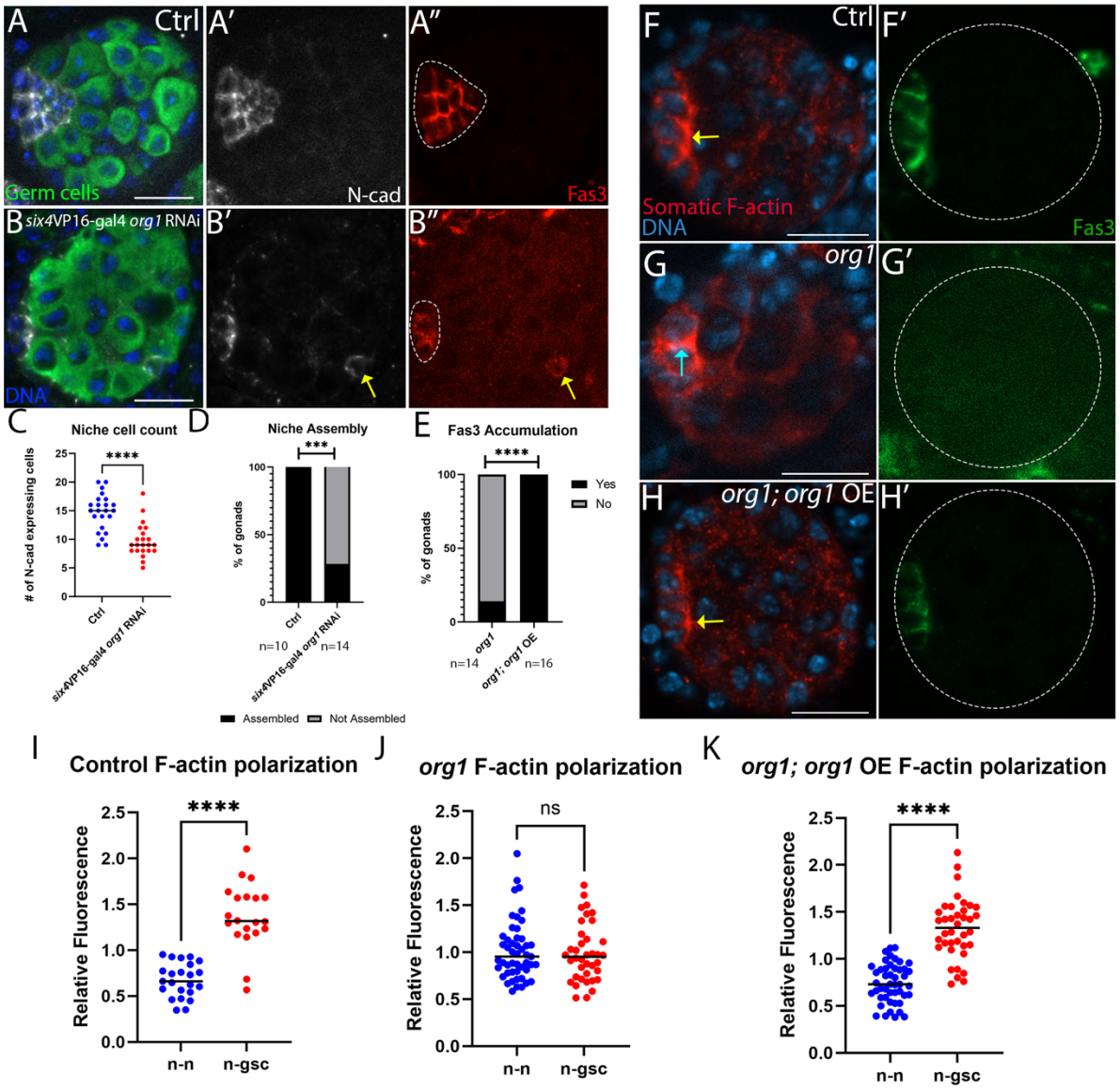

Figure 3. *org1* is required SGP intrinsically for niche identity and assembly. (A, A', A'') Control gonads with N-cad (white) and Fas3 (red) accumulating at the anterior. (B, B', B'') *org1* knockdown with six4gal4VP16 gonads showed fewer niche cells that accumulate N-cad (white) and Fas3 (red) at the anterior, with displaced niche cells (yellow arrow). Brightness and contrast were adjusted in A" and B" to enable visualization of Fas3. (C) Quantification of niche cell count per gonad in *org1* knockdown ($p<0.0001$, Ctrl n=23 gonads; six4VP16-gal4 *org1* RNAi n=22 gonads, Mann-Whitney Test). (D) Quantification of niche assembly in six4VP16-gal4 *org1* RNAi ($p= 0.0006$, Ctrl n= 10 gonads; *org1* RNAi n=14 gonads, Fisher's Exact Test) (E) Quantification of Fas3 accumulation in *org1* rescue niches ($p<0.0001$, *org1* n= 14 gonads; *org1; org1* OE n= 16 gonads, Fisher's Exact Test). (F-H) Yellow arrows indicate niche-GSC F-actin interfaces and blue arrows indicate niche-niche F-actin interfaces. (F, F') Control gonad with Fas3 (green) accumulating at the anterior. (G, G') *org1* knockout mutant gonad with no Fas3 (green) accumulation. (H, H') *org1* knockout mutant with *org1* overexpression in somatic gonadal cells (red) with rescued Fas3 (green) accumulation. (F-H) arrows indicate F-actin enrichment at

249 specific SGP interfaces. (I) Quantification of F-actin polarization in control gonads (p<0.0001, n-
250 n interfaces n=23; n-gsc interfaces n=20, from 7 gonads, Mann-Whitney Test). (J) Quantification
251 of F-actin polarization in *org1* mutants (not significant, n-n interfaces n=49; n-gsc interfaces
252 n=38, from 14 gonads, Mann-Whitney Test). (K) Quantification of F-actin polarization in *org1*
253 mutant rescued gonads (p<0.0001, n-n interfaces n=47; n-gsc interfaces n=38, from 16 gonads,
254 Mann-Whitney Test). Scale bars, 10 um.
255

256 ***org1* is important for niche to stem cell communication.**

257 Given the defects in niche identity and organization seen when *org1* is compromised, we tested
258 if the function was compromised without *org1*. We used known steady state niche signaling
259 pathways and centrosome position to assay for niche function deficits (Leatherman & DiNardo,
260 2010; Kiger et al., 2001; Tulina & Matunis, 2001; Yamashita et al., 2003, 2005). Stat
261 accumulates in GSCs in response to niche signals (Chen et al., 2018; Kiger et al., 2003), and
262 we measured reduced Stat accumulation in GSCs from whole organism *org1* mutants (Figure
263 4A-4B', 4G). Niche cells are also responsible for sending Hh signals to prospective CySCs to
264 enable their self-renewal (Michel et al., 2012; Amoyel et al., 2013).We examined localization of
265 Patched, a Hh receptor that accumulates in vesicles in the niche and CySCs in response to
266 signaling (Amoyel et al., 2013; Michel et al., 2012; Wingert & DiNardo, 2015) (Fig 4C-4D'). *org1*
267 mutants had significantly reduced Patched accumulation in the niche and never accumulated
268 Patched in nearby somatic cells (Figure 4C-4D', 4H).
269

270 We also tested stem cell behavior in the absence of *org1*. During normal GSC divisions, the
271 mother centrosome is anchored close to the niche-germline stem cell interface and thereby
272 enables GSC divisions perpendicular to the niche (Yamashita et al., 2003). Gonads from *org1*
273 null animals showed defects in centrosome proximity to the niche interface, with large gaps
274 between the niche and the centrosome (Figure 4E-4F', 4I). Together, our data suggest that *org1*
275 is required to generate niche cells capable of communication with stem cells, further supporting
276 a role for *org1* in niche cell specification.
277

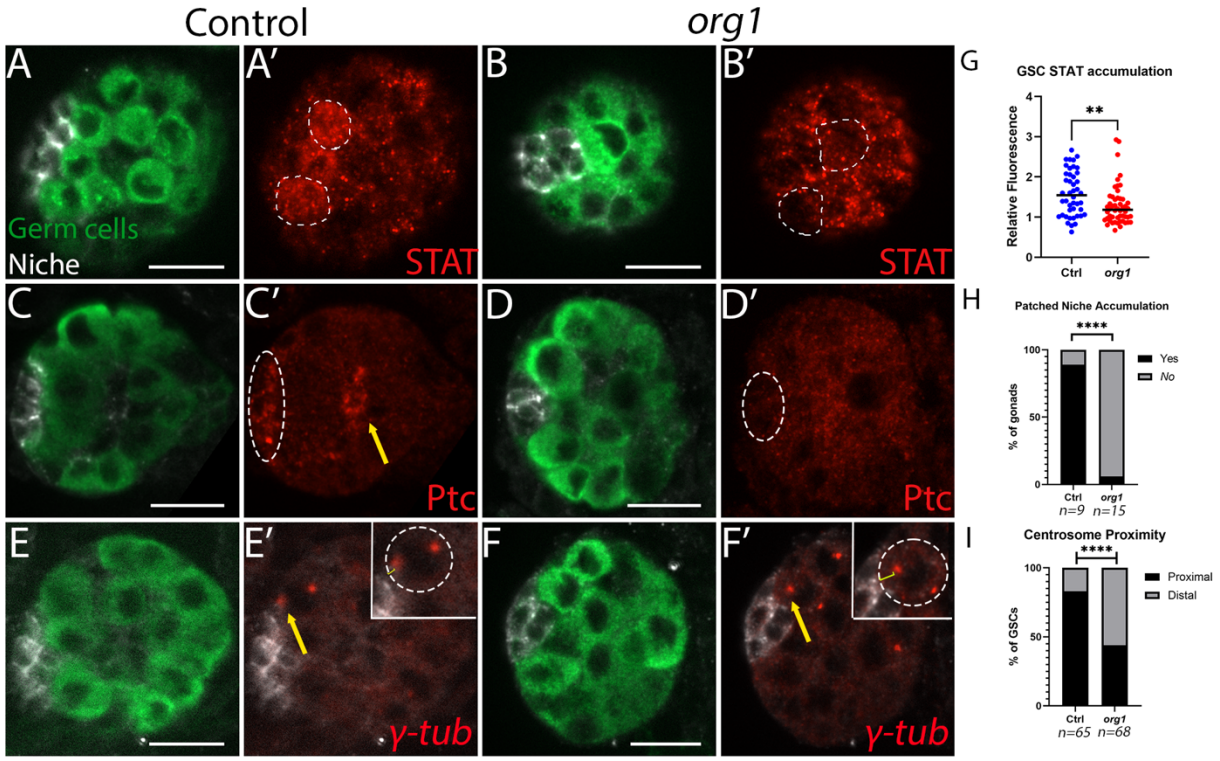

Figure 4. *org1* is important for niche to stem cell communication. (A, A') STAT (red) accumulated in germline stem cells (dotted line) in control gonads, but (B, B') not in *org1* mutant germline stem cells. (C, C') Hedgehog signaling receptor Patched (red) accumulated in the niche (white dotted line) and Cyst stem cells (yellow arrow). (D, D'') Patched did not accumulate in *org1* mutant gonads in the niche or cyst stem cells. (E, E') In control gonads, the nearest centrosome in each GSC was located very close to the interface with the niche (yellow bracket). Insets show germline stem cells outlined in white, and the niche boundary (Fas3, white). (F, F') In *org1* mutant gonads, the nearest centrosome in each GSC was located with greater distance from the niche interface (yellow bracket). (E', F') Nearest centrosomes are indicated by a yellow arrow and insets show centrosome pairs. (G) Quantification of STAT accumulation (p= 0.0041, Ctrl n=44 niche cells from 11 gonads; *org1* n=52 niche cells from 16 gonads, Mann-Whitney Test). (H) Quantification of Patched accumulation in the niche (p<0.0001, Ctrl n=9 gonads; *org1* n= 15 gonads, Mann-Whitney Test). (I) Quantification of centrosome anchoring (p<0.0001, Ctrl n=65 germline stem cells from 18 gonads; *org1* n= 68 germline stem cells from 21 gonads, Fisher's Exact Test). For all panels: Vasa (green), N-cad (white), scale bars, 10 um.

islet* regulates niche cell specification downstream of *org1

Our previous work has shown that *islet* is expressed downstream of Vm signals Slit and FGF and is important for niche assembly (Anllo & DiNardo, 2022). Here, we show *org1* is also expressed downstream of Slit and FGF and has a role in niche assembly (see Figure 1,3). Because *org1* is known to induce *islet* expression in embryonic muscle (Boukhatmi et al., 2014), we next tested if *org1* regulated *islet* in the embryonic gonad. Indeed, we saw that Islet was no

longer enriched in *org1* mutant niche cells (Figure 5A-5C). We also hypothesized that if *org1* is regulating *islet*, we would see Islet accumulation in the additional niche cells specified with our SGP lineage specific *org1* overexpression. Indeed, we saw that additional niche cells at the anterior also accumulated Islet (Figure 5D-5F). These data indicate that Islet accumulates in response to *org1* expression.

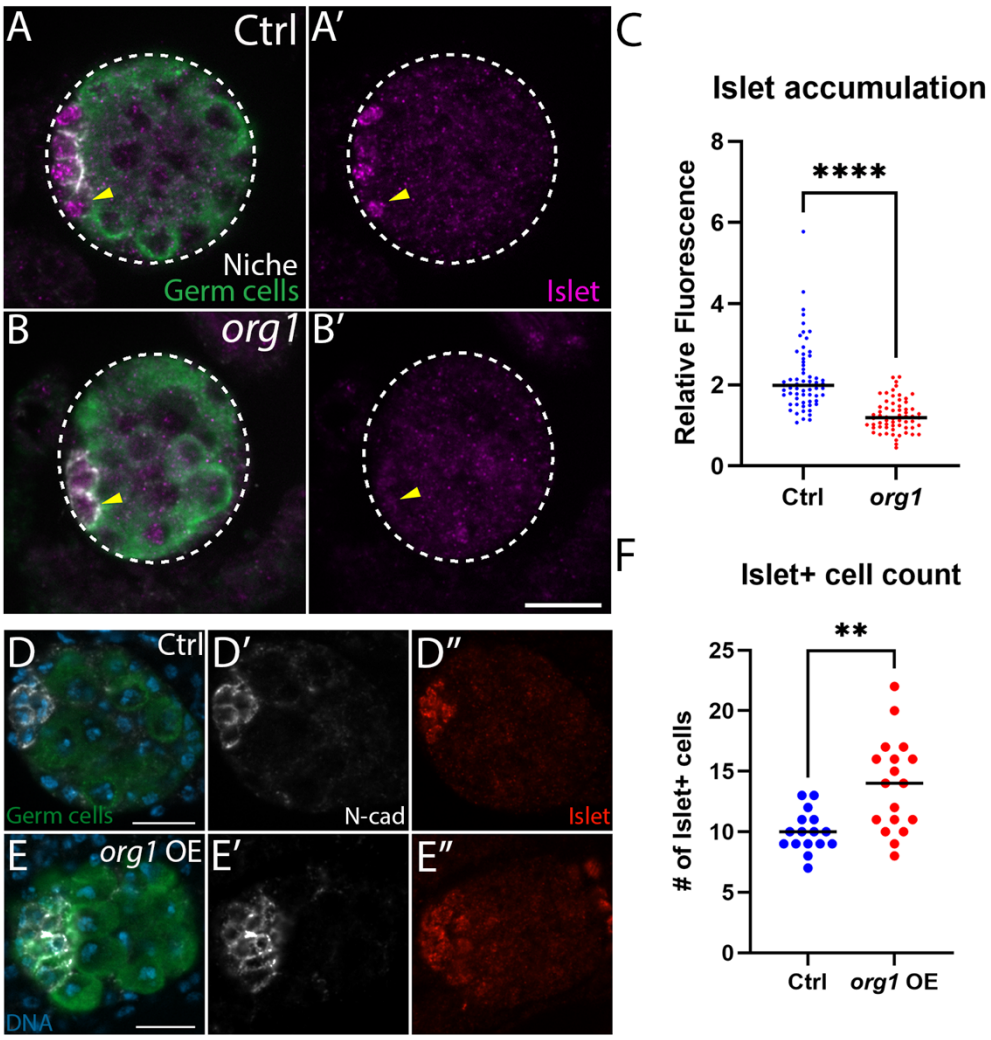

Figure 5. *org1* is important for Islet accumulation. (A, B) Germ cells (Vasa, green), Niche (Ncad, white), DNA (Hoechst, blue). (A, A') Control gonads showed Islet (magenta) accumulation enriched in the niche. (B, B') *org1* mutant gonads exhibited diminished Islet accumulation. (C) Islet accumulation quantification in niche cells ($p<0.0001$, Ctrl n=63 from 21 gonads; *org1* n=63 from 21 gonads, Mann-Whitney Test). (D, D', D'') Control gonads with N-cad (white) and Islet (red) accumulating in niche cells. (E, E', E'') *org1* overexpressing gonad with additional niche cells (white) that also accumulated Islet (red). (F) Quantification of number of

314 Islet accumulating cells (p= 0.0013, Ctrl n=16 gonads; *org1* OE n=18 gonads, Mann-Whitney
315 Test). Scale bars, 10 um.

316

317 The accumulation of Islet in response to *org1* parallels the transcriptional cascade that specifies
318 embryonic alary muscle specification (Boukhatmi et al., 2014). We thus hypothesized that *islet*
319 may also play a role in specifying niche cells in addition to the role we previously identified
320 during assembly (Anllo & DiNardo, 2022). To test this hypothesis, we quantified the number of
321 Fas3 accumulating niche cells in *islet* mutants compared to controls. Indeed, we counted fewer
322 Fas3 accumulating cells in *islet* mutants, supporting our hypothesis (Figure 6A-6C).

323 To further support a role for *islet* in niche specification downstream of *org1,* we asked whether
324 we could rescue *org1* mutant niche cell number with *islet* overexpression. We overexpressed
325 *islet* with our SGP lineage-specific driver *six4*-gal4. In gonads with both the *org1* mutation and
326 SGP-specific restoration of *islet*, we saw increased numbers of niche cells compared to *org1*
327 mutants alone (Figure 6G-6J'), supporting an ability to rescue niche cell identity. While niche cell
328 number increased with *islet* overexpression, this number was still not fully rescued to control
329 levels, and *islet* overexpression in control genetic backgrounds does not significantly increase
330 niche cell number (Figure 6G). These results suggest that while *islet* is clearly important for
331 niche identity, its expression alone is not fully sufficient to induce niche cell fate. Taken together,
332 our results support a role for *islet* in niche cell specification and suggest that it acts downstream
333 of *org1* in this role.

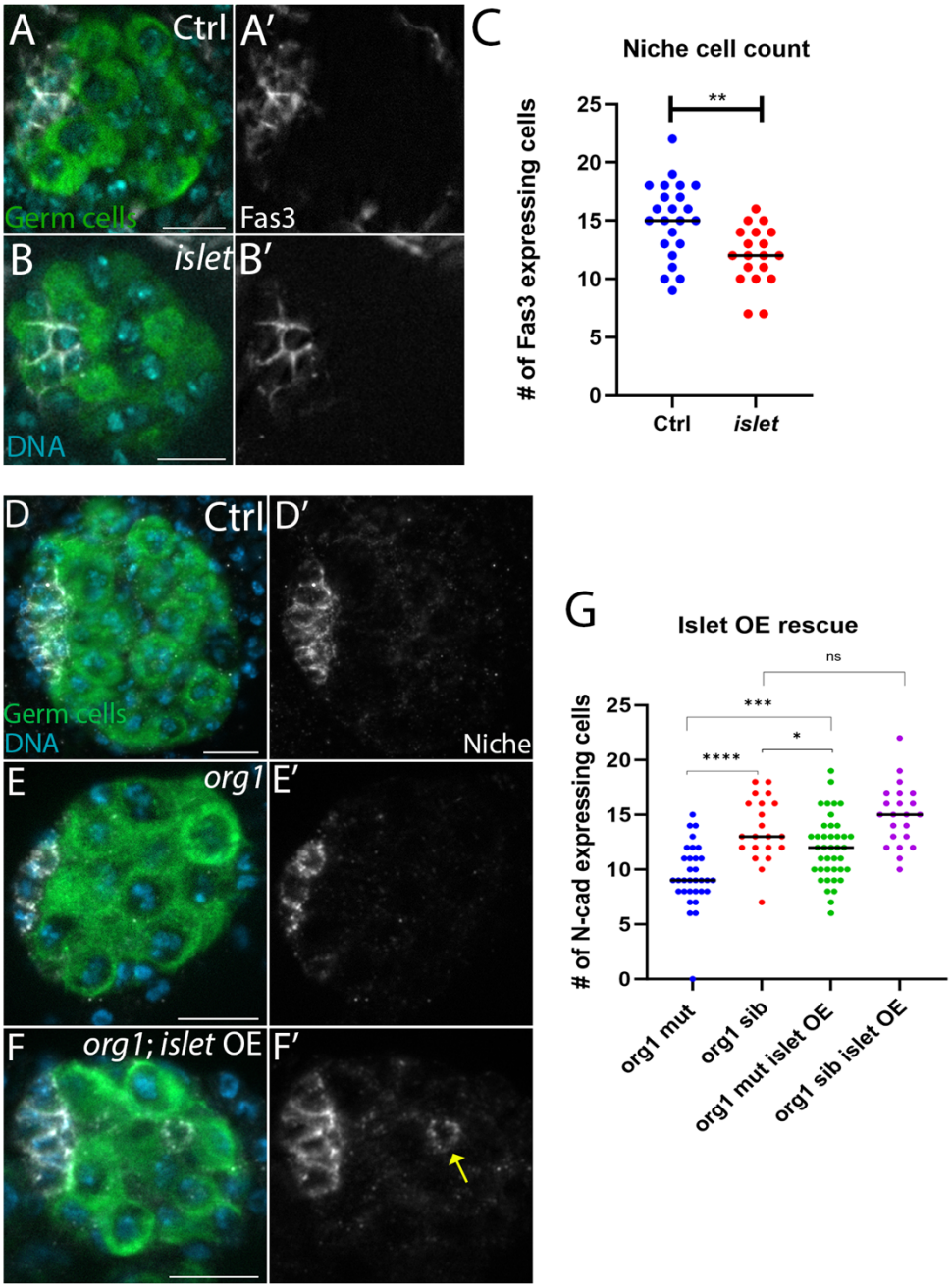

334

335 **Figure 6. *islet* regulates niche cell specification downstream of *org1***. Germ cells (Vasa,
336 green), DNA (Hoechst, blue), Niche cells (white). Scale bars, 10 um. (A, A') Control gonads with
337 niche (Fas3, white) at the anterior. (B, B') *islet* mutant gonad with disrupted niche (Fas3, white)
338 at the anterior. (C) Quantification of niche cells per gonad in *islet* mutants (p= 0.0019, Ctrl n=23
339 gonads; *islet* n=19 gonads, Mann-Whitney Test). (D, D') Control gonads with N-cad (white) and
340 Islet (red) accumulating in niche cells. (E, E') *org1* mutant gonad with fewer niche cells
341 accumulating N-cad at the anterior. (F, F') An *org1* mutant with *islet* overexpression in somatic
342 gonadal cells had more niche cells than *org1* mutants, and a displaced niche cell (yellow arrow).
343 (G) Number of niche cells per gonad for *org1* rescue with *islet* overexpression experiments
344 (*org1* mut vs *org1* sib, p<0.0001, *org1* mut n=32 gonads; *org1* sib n=21 gonads. *org1* mut vs

org1 mut *islet* OE, p=0.0005, *org1* mut n=32 gonads; *org1* mut *islet* OE n=40 gonads. *org1* sib vs *org1* mut *islet* OE, p=0.0338, *org1* sib n=21 gonads; *org1* mut *islet* OE n=40 gonads. *org1* sib vs *org1* sib *islet* OE, not significant, *org1* sib n=21 gonads; *org1* sib *islet* OE n=22 gonads) Mann-Whitney Tests. Scale bars, 10 um.

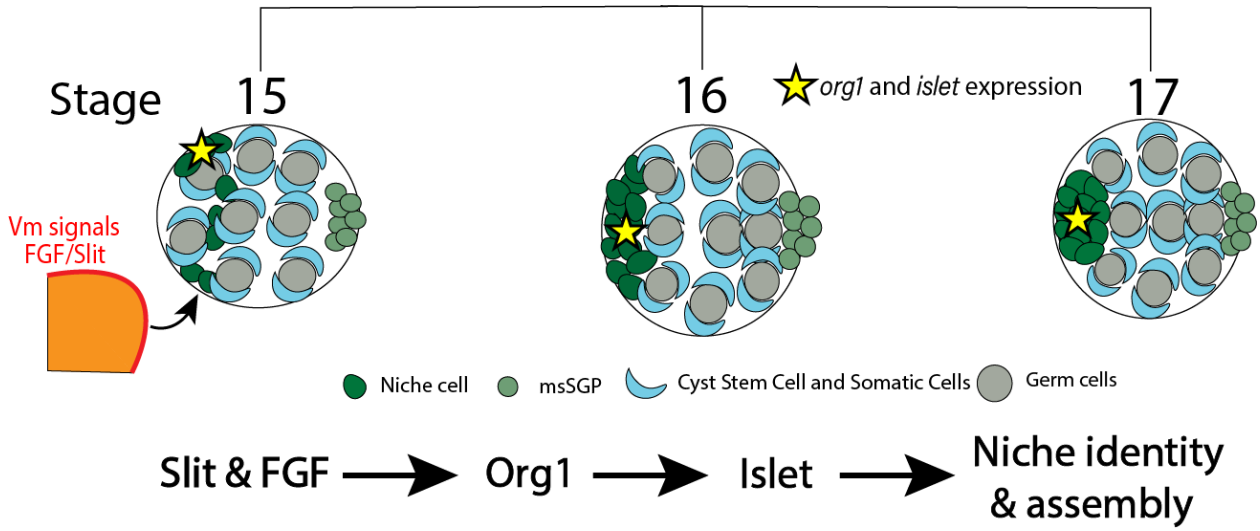

Figure 7. Predicted model of establishment of niche identity and assembly. Visceral muscle signals Slit and FGF regulate *org1*. *org1* functions to regulate *islet* for niche identity and assembly.

355 **Discussion:**

356 An impressive body of work has explored stem cell and niche functions (Anllo & DiNardo, 2022;
357 Kaestner et. al., 2019; Losick et al., 2011; Morrison & Spradling, 2008; Sato et al., 2011; Vida et
358 al., 2024; Warder et. al., 2024; Wei et al., 2023; Yamashita et al., 2005), yet how niche cells
359 acquire their identity and are positioned to properly regulate resident stem cells is largely
360 unknown. Prior to our work, Notch signaling and a downstream transcriptional regulator, *traffic*
361 *jam,* were identified as inputs to *Drosophila* testis niche identity (Kitadate & Kobayashi, 2010;
362 Okegbe & DiNardo, 2011; Wingert & DiNardo, 2015). These inputs are first induced by early
363 contact with the developing gut (Okegbe & DiNardo, 2011). Our previous work studying extrinsic
364 signals important for niche establishment has linked niche assembly with niche function in this
365 system (Anllo & DiNardo, 2022), and prior work has linked niche cell identity and assembly
366 (Wingert & DiNardo, 2015). Here, we have identified a novel regulator that further supports a
367 connection between the processes of niche identity and assembly, the Tbx1 ortholog *org1*. We
368 show that *org1* is expressed in response to niche assembly cues from neighboring visceral muscle
369 (Anllo & DiNardo, 2022; this work). In addition, we have defined *islet* as a regulator of niche
370 identity operating downstream of *org1* (Fig 7, model). The combination of these factors suggests
371 that niche assembly and identity are controlled through overlapping processes. Our work
372 addresses a knowledge gap in mechanisms specifying functional stem cell niches, revealing
373 signals that control both niche identity and proper assembly of a compartmentalized niche.

374

375 **Testis niche identity and assembly are linked**

376 Our previous work showed that the Visceral muscle signals Slit and FGF are required for niche
377 assembly. When niche assembly was compromised, niche function was also disrupted even
378 though these manipulations did not directly affect niche identity (Anllo & DiNardo, 2022).
379 Previous work suggested a connection between niche identity and assembly (Wingert &
380 DiNardo, 2015). In response to the niche specification signal Notch, the Maf transcription factor

381 *traffic jam* (*tj*) is downregulated. *traffic jam* mutants specify additional niche cells that do not
382 express all niche identity markers, and as a result do not assemble at the anterior (Wingert &
383 DiNardo, 2015). Interestingly, activating other requirements of niche identity such as Bowl
384 places the additional *tj* mutant niche cells at the gonad anterior (Wingert & DiNardo, 2015;
385 DiNardo et al., 2011). This suggests that reduction of *traffic jam* alone is not sufficient for niche
386 assembly at the anterior, supporting a role for additional regulators specifying niche cells
387 capable of assembly. Perhaps the signals necessary for anterior assembly (Slit and FGF) are
388 unable to be received by ectopic niche cells in *tj* mutants.
389
390 We have shown that niche assembly signals Slit and FGF are important for regulating the novel
391 niche identity regulator *org1*. Gonads with compromised *org1* show fewer cells expressing niche
392 identity markers, and assembly defects in which some niche cells do not arrive at the anterior
393 (this work). *traffic jam* mutants show additional cells expressing niche identity markers, and
394 these cells are also located in positions away from the gonad anterior (Wingert & DiNardo,
395 2015). Together, these data link proper specification of niche identity with anterior assembly.
396
397 Interestingly, the loss of *slit* and *fgf* regulators do not completely mimic phenotypes seen in *org1*
398 mutants. For instance, Vm signaling mutants are capable of accumulating Fas3, whereas *org1*
399 mutants do not. We detect residual Org1 accumulation in niche cells from *slit* and *fgf* mutants
400 (Figure 1) suggesting that additional regulators are impacting *org1* expression. We suspect that
401 while Slit and FGF both regulate *org1*, Slit and FGF signaling have a primary role in facilitating
402 niche cell anterior placement, while *org1* has a primary function in specifying niche cell identity.
403
404 ***islet* has dual roles in niche identity and assembly downstream of *org1***
405 To further link niche identity and assembly, we present an exciting new role for the transcription
406 factor *islet* in niche cell specification in addition to the role we previously revealed for *islet* in niche

407 assembly. Together with our previous study, this work reveals that Visceral muscle signals induce
408 both *org1* and *islet* expression in niche cells (Anllo & DiNardo, 2022; this work). In addition, we
409 show that *org1* regulates *islet* in the niche, as *org1* mutant niches lack Islet, and niche cell
410 numbers are increased by overexpressing *islet* in SGPs in an *org1* mutant background. These
411 data support the model of a transcriptional cascade regulating *islet* first through Vm signals
412 inducing *org1,* which in turn induces *islet* expression (Figure 7). Interesting questions that remain
413 include identifying what other *org1* targets contribute to niche specification along with *islet*, and
414 revealing how *islet* influences the number of niche cells that accumulate Fas3 and N-cad.
415
416 The detection of dispersed, unassembled niche cells in our *six4*VP16-gal4 driven *org1* RNAi was
417 unexpected. It is reasonable to suggest earlier and stronger knockdown driving *org1* RNAi with
418 the enhanced *six4*VP16-Gal4 driver compared to that observed with *six4*-Gal4. Since we only
419 observed assembly defects under the presumed stronger conditions, we infer that *org1* has a
420 primary role in niche cell identity and a secondary role in niche assembly.
421
422 ***org1* regulates testis niche identity**
423 In alignment with Tbx1 orthologs and their conserved role in specifying mesodermal cell types,
424 we found it fitting to test if *org1* had a role in specifying the mesodermally-derived niche cells.
425 Using the niche identity markers Fasciclin3 (Fas3) and *hedgehog* (*hh*), we saw that *org1*
426 mutants were unable to properly accumulate these markers (Le Bras & Van Doren, 2006;
427 Okegbe & DiNardo, 2011). *hh* and its expression have been linked to niche assembly
428 downstream of Notch (Wingert & DiNardo, 2015). Using the *hh*-lacZ reporter, we detected high
429 levels of *hh* expression in the niche, and low levels of expression in SGPs outside the niche
430 (Figure S2). While we find that *hh* expression is not solely restricted to the niche in the
431 embryonic gonad as it is in the adult (Amoyel et. al., 2013), our ability to detect higher *hh*

432 expression in niche cells enables us to use its upregulated expression as a reliable marker for
433 niche identity.
434
435 There are residual niche cells in *org1* mutants, which suggests that other inputs of niche identity
436 are partly active. It has been previously described that Notch signaling is necessary for
437 specifying niche cells (Kitadate & Kobayashi, 2010; Okegbe & DiNardo, 2011). The average
438 number of niche cells in Notch mutants is far fewer than we see in *org1* mutants, which
439 suggested to us that *org1* is either one of multiple effectors downstream of Notch or involved in
440 a parallel niche specification mechanism. One of the downstream effects of Notch signaling in
441 specifying niche cells is to downregulate Traffic jam (Tj) accumulation in these cells. Previously,
442 it was not known when downregulation of *traffic jam* began in prospective niche cells (Wingert &
443 DiNardo, 2015). We detected downregulation of *tj* coinciding with the beginning of *org1*
444 expression in prospective niche cells after gonad coalescence. Since *org1*-expressing cells had
445 lowered levels of Tj, we considered whether *org1* might repress Tj. However, we have shown
446 that Tj is not regulated by *org1* (Figure S2). Alternatively, Tj might block *org1* expression. This
447 relationship could explain the higher accumulation or Org1::GFP we detect in SGPs with
448 reduced Tj (Figure 1B-B'', yellow arrows). Future work should assess whether Tj regulates *org1*
449 downstream of Notch.
450
451 Our work has established *org1* as a novel regulator of identity and assembly during testis niche
452 establishment. Multiple factors identified in the *Drosophila* testis stem cell niche have translated
453 into other systems, including a role for Notch in niche specification (Zamfirescu et al., 2022).
454 Because of the numerous cell biological concepts elucidated in this niche that have translated to
455 other systems, our work lays the foundation for future studies to investigate a conserved
456 capacity of Tbx1 to specify gonadal mesoderm or niche cell fate.
457

458 **Methods:**

459 **Embryonic gonad dissection and immunostaining:**

460 Embryos were collected for 2 hours and then aged for 20-22 hours in a humidified chamber at 25
461 C to stage 17. Embryos were then sorted for mutant and control genotypes using fluorescently
462 marked balancer chromosomes (FM7DfdYFP or TM6DfdGFP). Sorted embryos were dissected
463 and immunostained as previously described (Anllo et. al. 2019). Dissected tissue was incubated
464 at 4C overnight with primary antibodies. Secondary antibodies were used at 3.75 ug/mL
465 (Alexa488, Cy3, or Alexa647; Molecular Probes; Jackson Immunoresearch) for 1.5-2 hours at
466 room temperature. DNA was stained with Hoechst33342 (Sigma) at 0.2-0.3 ug/mL for 6 minutes.
467

468 We used goat anti Vasa 1:800 (Santa Cruz Biotech -Discont.); rabbit anti Vasa 1:5000 (BosterBio
469 DZ41154); mouse anti Fasciclin III 1:50 (DSHB AB_528238); rat anti N-cadherin 1:20 (DSHB
470 AB_528121); rat anti E-cad 1:20 (DSHB AB_528120); rabbit anti Stat92E 1:200 (gift from E. Bach,
471 NYU); rabbit anti RFP 1:500 (Abcam ab62341); mouse anti Islet 1:200 (DSHB AB_528313);
472 guinea pig anti Traffic jam 1:10,000 (Gift from D. Godt); rat anti Org-1 1:200 (gift from C. Schaub);
473 mouse anti Gamma Tubulin 1:200 (Sigma AB_477584); chicken anti Beta-gal 1:1000 (Abcam
474 ab9361-250); mouse anti Patched 1:50 (DSHB AB_528441); and chicken anti GFP 1:1000 (Aves
475 labs AB_2307313).
476

477 Tissue was imaged using a Zeiss AxioImager.Z1 microscope equipped with an ApoTome.2, X-
478 cite Xylis fluorescent light source, and Axiocam 705 mono camera, using 40x 1.2 N.A. plan apo
479 lens. Org1::GFP reporter images in Stage 15 embryos were obtained with a Crest X-Light V3
480 spinning disk confocal on an Olympus IX83 platform with a 60x 1.3 N.A. plan apo silicone oil
481 immersion objective.
482
483

484 ***Drosophila* strains:**

485 All *Drosophila* lines used are listed in the Key Resources Table. *org1[OJ407]* is a null allele lacking
486 the translation initiation codon and T-box domain (Schaub et al., 2012). Org1::GFP is a bacterial
487 artificial chromosome including the *org1* coding sequence and nearby genetic regulatory elements
488 upstream of an in-frame GFP sequence (Kudron et al., 2018). *slit[2]* is a null allele with no
489 detectable protein product (Battye et. al., 2001; Nusslein-Volhard et. al., 1984). To remove *pyr*
490 and *ths* FGF ligands together, we used a small chromosomal deficiency, Df(2R)BSC25, which
491 completely deletes the genes encoding both ligands (Stathopoulos et al., 2004).

492

493 **Identification of male gonads, and the niche:**

494 We identified male gonads by the presence of male specific SGPs at the posterior (De Falco et.
495 al., 2003) which were visualized with Vasa (BosterBio) or six4moeGFP (Sano et al., 2012).
496 Additionally, male gonads can be identified by the fact that they have more proliferative germ cells
497 and therefore have more germ cells than female gonads (Anllo et. al., 2019; Wawersik et. al.,
498 2005). Niches in stage 17 embryos were identified via immunofluorescence by niche cell specific
499 accumulation of Fasciclin 3 (DSHB AB_528238), or enrichment of N-cadherin (DSHB
500 AB_528121) or E-cadherin (DSHB AB_528120).

501

502 **Characterization of niche phenotypes:**

503 When assessing morphology and proper assembly of the niche, we characterized a niche as
504 either “assembled” or “unassembled”. “Assembled” niches show all niche cells contacting one
505 another at the gonad anterior and have clearly smoothened cell boundaries around the niche
506 periphery. “Unassembled” niches have niche cells anterior and at the gonad periphery, but with
507 irregular boundaries, and/or have dispersed niche cells that are not contacting the anterior cluster
508 of niche cells.

509

510

511 **Quantification of niche cell count:**

512 When quantifying the number of cells that express N-cad, Fas3, or any other niche marker, we
513 use the ImageJ Cell Counter Plugin to record cells that we counted manually. A niche cell will
514 accumulate Fas3 when in contact with other niche cells and will accumulate N-cad on all
515 interfaces. Niche cells that are counted with either Fas3 or N-cad are co-labeled with a nuclear
516 marker such as Traffic jam or Hoechst, to enable clear identification of distinct cells. Dispersed
517 niche cells that accumulate Fas3 do not show polarized enrichment to specific cell interfaces.

518

519 **Quantification of normalized niche cell expression/accumulation:**

520 When quantifying accumulation of proteins and reporters of gene expression, we used ImageJ
521 software to measure mean gray value fluorescence intensity within regions of interest (ROIs). We
522 selected ROIs including a circular region within somatic cell boundaries, using either Fas3 or N-
523 cad immunofluorescence to delineate niche cell boundaries and Hoechst dye to delineate nuclei.
524 ROIs were in a single Z plane in which the relevant cell was in focus. For each gonad, 3 niche
525 cell ROIs were measured. To quantify background fluorescence, an ROI was selected to
526 encompass the unlabeled region of a single germ cell within each gonad, and a separate
527 background ROI drawn from a region where no tissue was present. Background-subtracted
528 fluorescence values for each niche cell were normalized, dividing by the background-subtracted
529 value from the neighboring unlabeled germ cell for the respective gonad. Relative fluorescence
530 values for each niche cell were plotted. Mann-Whitney tests were used to evaluate comparisons.

531

532 **Quantification of fluorescence at cell junctions:**

533 To quantify fluorescence intensity of F-actin between cell interfaces, we used ImageJ software to
534 measure mean gray value fluorescence intensity within regions of interested (ROIs). ROIs were
535 either niche-niche interfaces or niche-GSC interfaces. We selected 4-pixel-wide segmented line
536 ROIs between niche cells and between niche cells and GSCs. 2-4 niche-niche and niche-GSC
537 interfaces were measured in every gonad using N-cad to visualize each interface. We measured

538 the mean fluorescence intensity of our Ftractin-tdTomato blindly with N-cad as a boundary. To
539 estimate background fluorescence, a separate ROI was drawn from a region where no tissue was
540 present. Background-subtracted fluorescence values for each niche cell were normalized, divided
541 by the background-subtracted average value of all cell interfaces. Relative fluorescence values
542 for each interface were plotted. Mann-Whitney tests were used to evaluate comparisons.
543
544 **Quantification of Stat accumulation:**
545 To quantify Stat accumulation, we stained gonads with a Stat antibody (E. Bach, 1:200) and used
546 ImageJ to measure the mean gray value fluorescence intensity within regions of interest (ROIs).
547 During dissections and staining, we used the phosphatase inhibitor PhosStop (Sigma –
548 Cat#4906845001). We selected ROIs including a circular region to sample germ cells, using Vasa
549 immunofluorescence as a marker to delineate cell boundaries. Whole germ cells were measured
550 in a single Z plane in which the relevant cell was in focus. We selected ROIs by only using the
551 germ cell marker to mark sample regions to avoid biased observations towards brighter or dimmer
552 fluorescence of Stat. For each gonad, we sampled all GSCs we could clearly identify and 3-7
553 neighboring germ cells in the second tier, further from the germline stem cells. After background
554 subtraction, we measured the ratio of Stat accumulation within each GSC relative to the
555 neighboring germ cell average for that gonad. Relative Stat enrichment values were plotted for
556 each GSC. We obtained measurements on sibling controls and in mutants for *org1*. Mann-
557 Whitney tests were used to evaluate comparisons.
558
559 **Centrosome anchoring quantification:**
560 To quantify changes in centrosome orientation, we focused on GSCs with two visible centrosomes
561 as judged by immunostaining for Gamma tubulin, indicating that they had advanced at least to
562 the G2 stage of the cell cycle (Chen et. al., 2018). We then scored the position of the centrosome
563 nearest to the GSC-niche boundary as marked by N-cad accumulation. As expected, in control
564 gonads, this nearest of the pair of centrosomes was most often directly adjacent to the interface

565 judged to be within one to two centrosome diameters (Figure 4I; Ctrl; 52 / 65 near centrosomes).
566 In contrast, in mutant gonads many centrosomes were positioned further from the interface (see
567 Fig I).
568

569 **Key Resources Table:**

Reagent Type	Designation	Source	Identifiers
Genetic reagent (D. melanogaster)	org1[OJ487]/ FM7DfdYFP or Y	Bloomington Drosophila Stock Center	Schaub et. al., 2012; RRID: BDSC_91555
Genetic reagent (D. melanogaster)	org1 RNAi (II)	Vienna Drosophila Stock Center	v104393
Genetic reagent (D. melanogaster)	UAS-org1	Bloomington Drosophila Stock Center	Schaub et. al., 2012; RRID: BDSC_92971
Genetic reagent (D. melanogaster)	*six4*-gal4/CyoDfdYFP; Dr/Tm3,sb	Anllo et al., 2019	
Genetic reagent (D. melanogaster)	*six4*VP16-gal4/CyoDfdYFP; Dr/TM3,Sb	Warder et al., 2024	
Genetic reagent (D. melanogaster)	w[*] ; P{w+ UAS-islet} on III	Bloomington Drosophila Stock Center	RRID:BDSC_39662
Genetic reagent (D. melanogaster)	ry[506], P{ry+}hhLacZ	Bloomington Drosophila Stock Center	RRID:BDSC_5530
Genetic reagent (D. melanogaster)	P-Dsix4-eGFP::Moesin	R. Lehmann	Sano et. al., 2012
Genetic reagent (D. melanogaster)	Pbac{org-1-GFP.FPTB}VK00033/ TM6C, Sb[1]	Bloomington Drosophila Stock Center	Kudron et al., 2018
Genetic reagent (D. melanogaster)	six4>ftractin tdTomato on II	Stephen DiNardo	RRID: BDSC_58989 UAS-ftractin tdTomato

Genetic reagent (D. melanogaster)	Df(2R)BSC25 – *fgf* mutant	Bloomington Drosophila Stock Center	RRID: BDSC_6865
Genetic reagent (D. melanogaster)	*slit[2]*	Bloomington Drosophila Stock Center	RRID: BDSC_3266 (Battye et. al., 2001; Nusslein-Volhard et. al., 1984)
Genetic reagent (D. melanogaster)	tupex4	S. Campuzano	FBal0216723; (Stathopoulos et al., 2004).
Antibody	Goat polyclonal anti-Vasa	Santa Cruz Biotechnology	RRID:AB_793880 Discontinued
Antibody	Mouse monoclonal anti Fasciclin III	Developmental Studies Hybridoma Bank	RRID:AB_528238
Antibody	Rabbit polyclonal anti STAT92E	E. Bach	
Antibody	Rabbit polyclonal anti RFP	Abcam	RRID:AB_945213
Antibody	Mouse monoclonal anti Islet	Developmental Studies Hybridoma Bank	RRID:AB_528313
Antibody	Guinea pig polyclonal anti Traffic jam	D. Godt	
Antibody	Rat anti Org-1	C. Shaub	
Antibody	Mouse monoclonal anti Gamma-tubulin	Sigma	RRID:AB_477584
Antibody	Rabbit Polyclonal anti Vasa	Boster Bio	DZ41154
Antibody	Chicken polyclonal anti Beta-gal	Abcam	ab9361-250
Antibody	Mouse Monoclonal anti Patched	Developmental Studies Hybridoma Bank	RRID: AB_528441
Antibody	Rat monoclonal anti CadN	Developmental Studies Hybridoma Bank	RRID: AB_528121
Antibody	Rat monoclonal anti CadE	Developmental Studies Hybridoma Bank	RRID: AB_528120
Antibody	Chick polyclonal anti GFP	Aves Labs	RRID: AB_2307313
Antibody	Alexafluor Secondary Antibodies (488, 647)	Molecular Probes	

Antibody	Cy3 Affinipure Secondary Antibodies	Jackson ImmunoResearch	RRID: AB_2307443
Chemical Compound, Drug	Hoechst	Sigma	Cat#33342; CAS Number: 875756-97-1
Chemical Compound, Drug	Normal Donkey Serum (NDS)	Jackson Immunoresearch Laboratories	RRID: AB_2337258
Chemical Compound, Drug	Ringers		doi:10.1101/pdb.rec12409
Chemical Compound, Drug	Heptane		
Chemical Compound, Drug	Propyl-gallate	Sigma Aldrich	SKU: P3130; CAS Number 121-79-9
Chemical Compound, Drug	Para-Formaldehyde (PFA), 16%	Electron Microscopy Sciences	Cat#15710
Chemical Compound, Drug	Phosphatase inhibitor (PhosphaSTOP)	Roche/Sigma	Cat#4906845001
Software, Algorithm	FIJI (Image J)	www.fiji.sc	
Software, Algorithm	Image J	www.imagej.nih.gov/ij/	
Software, Algorithm	Graphpad Prism	Graphpad Software	RRID:SCR_002798
Software, Algorithm	Axio-Vision Imaging Software	Zeiss	v4.8.1
Software, Algorithm	Adobe Photoshop	https://www.adobe.com/uk/products/photoshop.html	RRID:SCR_014199

Equipment	Zeiss Axioimager.Z1	Zeiss	
Equipment	ApoTome.2	Zeiss	
Equipment	Xcite Xylis	Zeiss	
Equipment	40x 1.2 NA objective	Zeiss	
Equipment	Leica M165FC	Leica	
Equipment	GFP Filter set ET470/ 40x; ET525/50m	Leica 10447408	

570

571

572 **Supplemental Figures:**

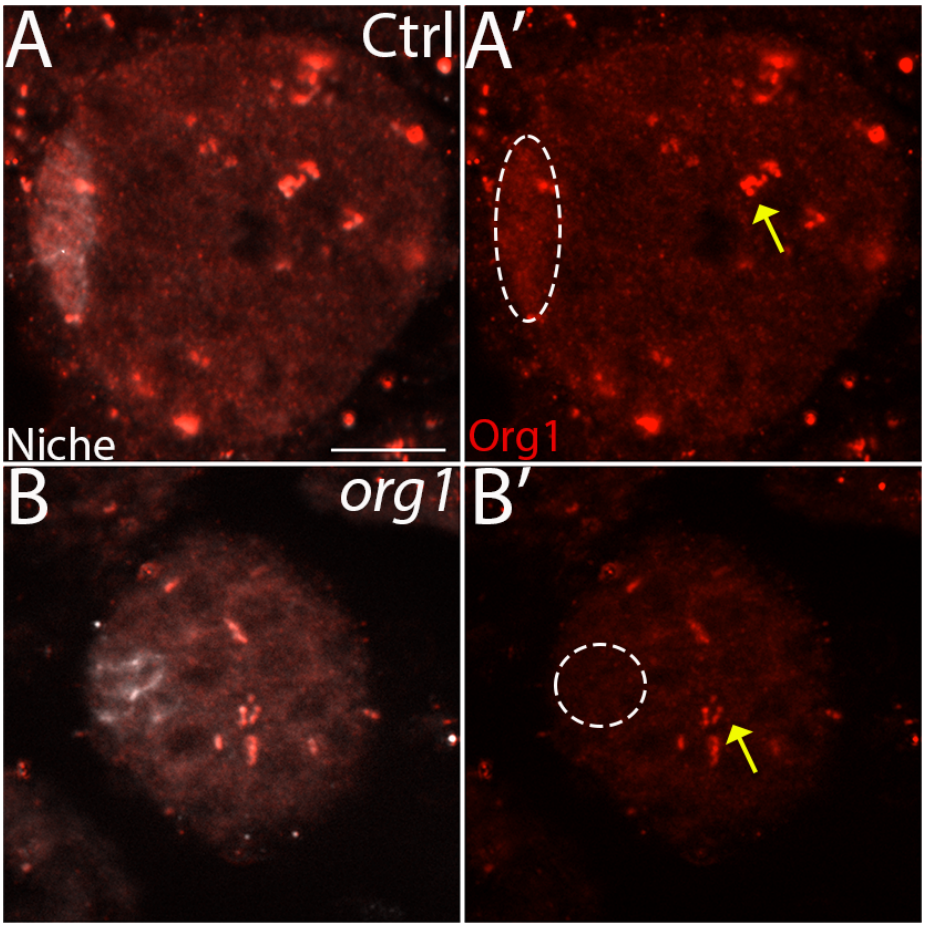

573

574 **Figure S1. Org1 antibody validation in *org1* mutants.** (A, A') Control gonads with Org1
575 accumulation (red) in the niche (Fas3, white) at the anterior, along with variable punctate signal
576 in other places in the gonad (yellow arrow). (B, B') *org1* mutant gonads with no Org1
577 accumulation (red) in the niche (white) at the anterior. Note that the variable punctate signal still
578 persists (yellow arrow) in the mutant and is thus spurious background and cannot be due to
579 Org1. Scale bars, 10 um.
580

581

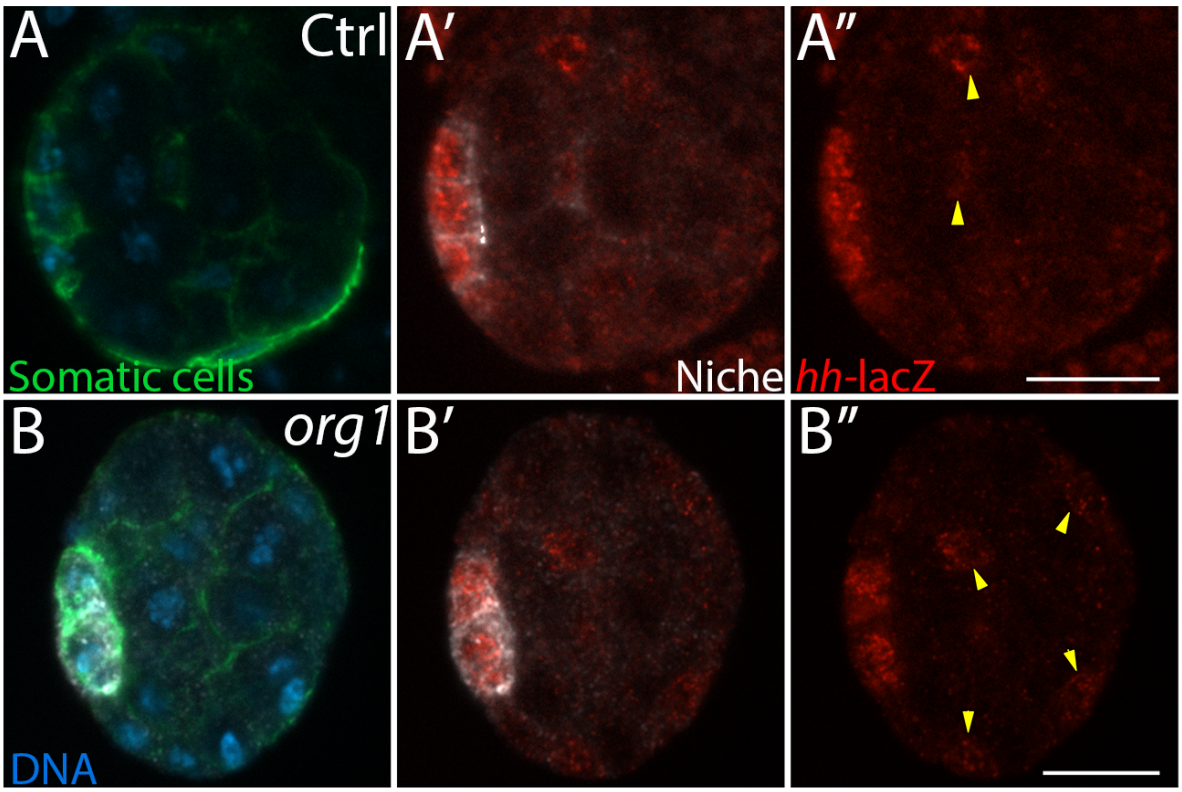

582

583 **Figure S2.** *hh* is expressed outside of the niche. Somatic cells (green), Niche (white), *hh*-lacZ
584 (red), DNA (blue). (A-A”) *hh*-lacZ reporter can be seen at high levels in niche cells, with lower
585 levels of expression outside of the niche (yellow arrows) in control gonads. (B-B”) *org1* mutant
586 gonads with low *hh*-lacZ expression in the niche (quantification in Fig 2), and outside of the
587 niche (yellow arrows).
588

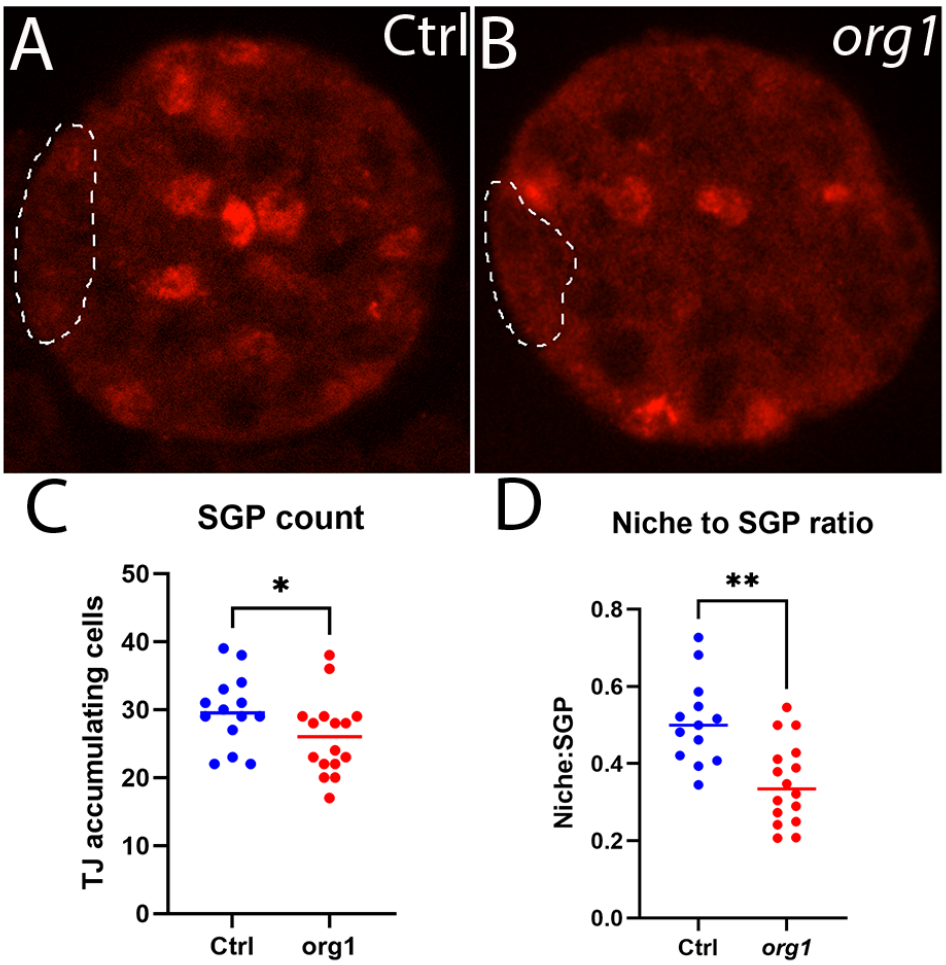

589

590 **Figure S3. *org1* mutants exhibit a lower ratio of niche cells relative to number of SGPs.**
591 (A) Control and (B) *org1* mutant gonads with Traffic jam accumulation. Niches are outlined with
592 dotted lines. (C) Quantification of number of Traffic jam accumulating SGPs indicated fewer
593 SGPs in *org1* mutants versus controls (p = 0.0399, Ctrl n= 14 gonads; *org1* n=16 gonads,
594 Mann-Whitney test). (D) Quantification of SGP to Niche cell ratio showed a lower ratio of niche
595 cells relative to SGPs in *org1* mutants (p = 0.0010, Ctrl n=13 gonads; *org1* n=16 gonads, Mann-
596 Whitney test). Scale bars, 10 um.
597

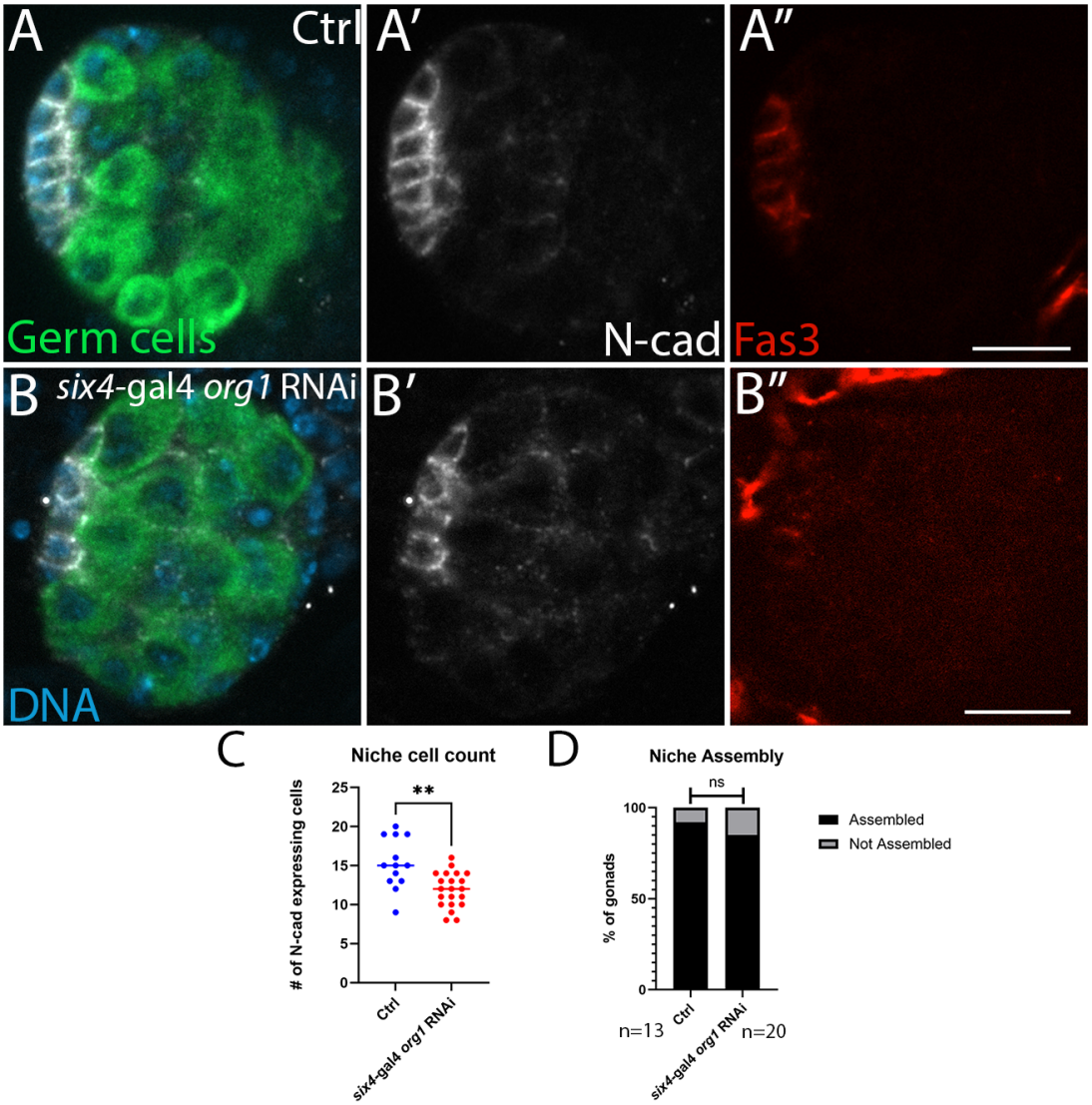

598

599 **Figure S4. *org1* RNAi with a Gal4 driver shows identity defects but not assembly defects.**
600 Germ cells (green), N-cad (white), Fas3 (red), DNA (blue). (A-A') Control gonads with
601 assembled niches and clear Fas3 accumulation. (B,B') *six4*gal4 > *org1* RNAi gonads with fewer
602 niche cells and reduced Fas3 accumulation. (C) Quantification of niche cell count in six4-gal4
603 *org1* RNAi gonads (p= 0.0022, Ctrl n=13 gonads; *six4*-gal4 *org1* RNAi n=21 gonads, Mann-
604 Whitney Test). (D) Quantification of assembly defects in six4-gal4 *org1* RNAi gonads (p> 0.99,
605 Ctrl n=13 gonads; *six4*-gal4 *org1* RNAi n=20, Mann-Whitney Test). Scale bars, 10 um.
606

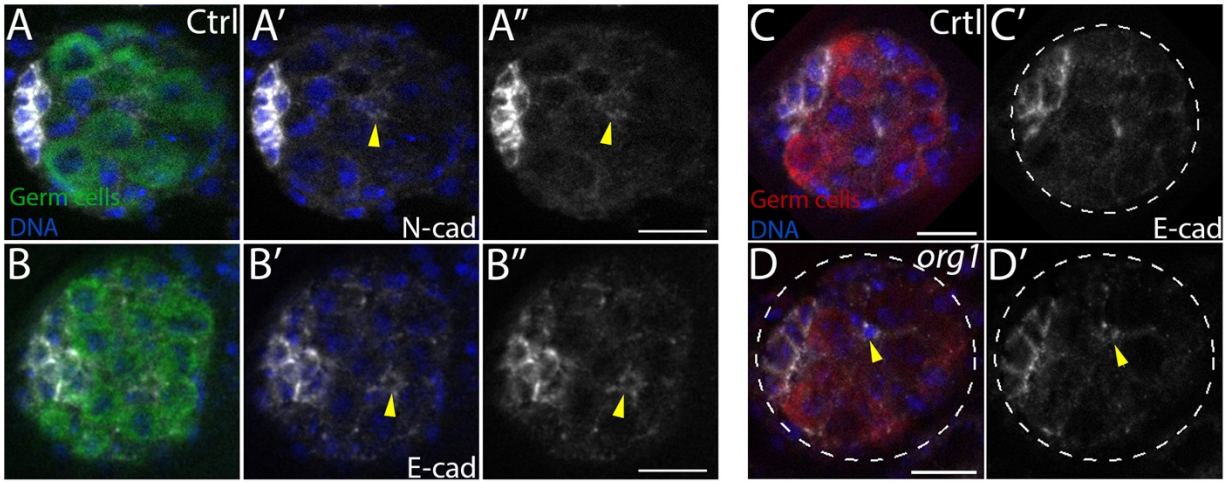

607

608 **Figure S5. N-cad and E-cad can be found spuriously in SGPs outside of the niche.** (A-B”)
609 Control gonads immunostained to show germ cells (green) and DNA (blue). (A) N-cad (white)
610 and (B) E-cad can be seen in an SGP (yellow arrow) outside of the niche but is not as enriched
611 at the cell cortex as in the anterior niche. (C-D’) Germ cells (red), E-cad (white), DNA (blue). (C,
612 C’) Control gonad with E-cad enriched in the cortex of niche cells. (D, D’) *org1* mutant gonad
613 with E-cad enriched to similar levels in a presumptive lost niche cell outside of the anterior niche
614 (yellow arrow). Scale bars, 10 um.
615

616 **References**

617 1. Amoyel, M., Sanny, J., Burel, M. and Bach, E. A. (2013). Hedgehog is required for CySC
618 self-renewal but does not contribute to the GSC niche in the Drosophila testis.
619 *Development (Cambridge)* 140, 56–65.
620 2. Anllo, L. and DiNardo, S. (2022). Visceral mesoderm signaling regulates assembly
621 position and function of the Drosophila testis niche. *Dev Cell* 57, 1009-1023.e5.
622 3. Anllo, L., Plasschaert, L. W., Sui, J. and DiNardo, S. (2019). Live imaging reveals hub
623 cell assembly and compaction dynamics during morphogenesis of the Drosophila testis
624 niche. *Dev Biol* 446, 102–118.
625 4. Battye, R., Stevens, A., Perry, R. L. and Jacobs, J. R. (2001). Repellent Signaling by Slit
626 Requires the Leucine-Rich Repeats.
627 5. Boukhatmi, H., Schaub, C., Bataillé, L., Reim, I., Frendo, J. L., Frasch, M. and Vincent,
628 A. (2014). An Org-1–Tup transcriptional cascade reveals different types of alary muscles
629 connecting internal organs in Drosophila. *Development (Cambridge)* 141, 3761–3771.
630 6. Boyle, M. and DiNardo, S. (1995). Specification, migration and assembly of the somatic
631 cells of the Drosophila gonad. *Development*.
632 7. Boyle, M., Bonini, N. and DiNardo, S. (1997). Expression and function of cliftin the
633 development of somatic gonadal precursors within the Drosophila mesoderm.
634 *Development*.
635 8. Chen, C., Cummings, R., Mordovanakis, A., Hunt, A., Mayer, M., Sept, D. and
636 Yamashita, Y. (2018). Cytokine receptor-Eb1 interaction couples cell polarity and fate
637 during asymmetric cell division.
638 9. de Cuevas, M. and Matunis, E. L. (2011). The stem cell niche: Lessons from the
639 Drosophila testis. *Development* 138, 2861–2869.
640 10. DeFalco, T. J., Verney, G., Jenkins, A. B., McCaffery, J. M., Russell, S. and Van Doren,
641 M. (2003). Sex-specific apoptosis regulates sexual dimorphism in the Drosophila
642 embryonic gonad. *Dev Cell* 5, 205–216.
643 11. DiNardo, S., Okegbe, T., Wingert, L., Freilich, S. and Terry, N. (2011). Lines and bowl
644 affect the specification of cyst stem cells and niche cells in the Drosophila testis.
645 *Development* 138, 1687–1696.
646 12. Herrera, S. C. and Bach, E. A. (2019). JAK/STAT signaling in stem cells and
647 regeneration: From drosophila to vertebrates. *Development (Cambridge)* 146,.
648 13. Herrera, S. C., Sainz de la Maza, D., Grmai, L., Margolis, S., Plessel, R., Burel, M.,
649 O'Connor, M., Amoyel, M. and Bach, E. A. (2021). Proliferative stem cells maintain

650 quiescence of their niche by secreting the Activin inhibitor Follistatin. *Dev Cell* 56, 2284-
651 2294.e6.
652 14. Inaba, M., Buszczak, M. and Yamashita, Y. M. (2015). Nanotubes mediate niche-stem-
653 cell signalling in the Drosophila testis. *Nature* 523, 329–332.
654 15. Jenkins, A. B., McCaffery, J. M. and Van Doren, M. (2003). Drosophila E-cadherin is
655 essential for proper germ cell-soma interaction during gonad morphogenesis.
656 *Development* 130, 4417–4426.
657 16. Kaestner, K. H. (2019). The Intestinal Stem Cell Niche: A Central Role for Foxl1-
658 Expressing Subepithelial Telocytes. *CMGH* 8, 111–117.
659 17. Kawase, E., Wong, M. D., Ding, B. C. and Xie, T. (2004). Gbb/Bmp signaling is essential
660 for maintaining germline stem cells and for repressing bam transcription in the
661 Drosophila testis. *Development* 131, 1365–1375.
662 18. Kiger, A. A., Jones, D. L., Schulz, C., Rogers, M. and Fuller, M. (2001). Stem Cell Self-
663 Renewal Specified byJAK-STAT Activation in Response to a Support Cell Cue. *Science*
664 *(1979)* 294, 2539–2542.
665 19. Kitadate, Y. and Kobayashi, S. (2010). Notch and Egfr signaling act antagonistically to
666 regulate germ-line stem cell niche formation in Drosophila male embryonic gonads. *Proc*
667 *Natl Acad Sci U S A* 107, 14241–14246.
668 20. Kudron, M. M., Victorsen, A., Gevirtzman, L., Hillier, L. W., Fisher, W. W., Vafeados, D.,
669 Kirkey, M., Hammonds, A. S., Gersch, J., Ammouri, H., et al. (2018). The modern
670 resource: genome-wide binding profiles for hundreds of Drosophila and Caenorhabditis
671 elegans transcription factors. *Genetics* 208, 937–949.
672 21. Le Bras, S. and Van Doren, M. (2006). Development of the male germline stem cell
673 niche in Drosophila. *Dev Biol* 294, 92–103.
674 22. Leatherman, J. L. and Di Nardo, S. (2008a). Zfh-1 controls somatic stem cell self-
675 renewal in the Drosophila testis and nonautonomously influences germline stem cell
676 self-renewal. *Cell Stem Cell* 3, 44–54.
677 23. Leatherman, J. L. and Di Nardo, S. (2008b). Zfh-1 controls somatic stem cell self-
678 renewal in the Drosophila testis and nonautonomously influences germline stem cell
679 self-renewal. *Cell Stem Cell* 3, 44–54.
680 24. Leatherman, J. L. and Dinardo, S. (2010). Germline self-renewal requires cyst stem cells
681 and stat regulates niche adhesion in Drosophila testes. *Nat Cell Biol* 12, 806–811.

682 25. Lee, S., Zhou, L., Kim, J., Kalbfleisch, S. and Schöck, F. (2008). Lasp anchors the
683 Drosophila male stem cell niche and mediates spermatid individualization. *Mech Dev*
684 125, 768–776.
685 26. Lenhart, K. F. and DiNardo, S. (2015). Somatic Cell Encystment Promotes Abscission in
686 Germline Stem Cells following a Regulated Block in Cytokinesis. *Dev Cell* 34, 192–205.
687 27. Li, L. and Xie, T. (2005). Stem cell niche: Structure and function. *Annu Rev Cell Dev Biol*
688 21, 605–631.
689 28. Li, H., Janssens, J., de Waegeneer, M., Kolluru, S. S., Davie, K., Gardeux, V., Saelens,
690 W., David, F. P. A., Brbić, M., Spanier, K., et al. (2022). Fly Cell Atlas: A single-nucleus
691 transcriptomic atlas of the adult fruit fly. *Science (1979)* 375,.
692 29. Li, G., Li, Z., Li, L., Liu, S., Wu, P., Zhou, M., Li, C., Li, X., Luo, G. and Zhang, J. (2023).
693 Stem Cell-Niche Engineering via Multifunctional Hydrogel Potentiates Stem Cell
694 Therapies for Inflammatory Bone Loss. *Adv Funct Mater* 33,.
695 30. Losick, V. P., Morris, L. X., Fox, D. T. and Spradling, A. (2011). Drosophila Stem Cell
696 Niches: A Decade of Discovery Suggests a Unified View of Stem Cell Regulation. *Dev*
697 *Cell* 21, 159–171.
698 31. Marcellini, S., Technau, U., Smith, J. C. and Lemaire, P. (2003). Evolution of Brachyury
699 proteins: Identification of a novel regulatory domain conserved within Bilateria. *Dev Biol*
700 260, 352–361.
701 32. Michel, M., Kupinski, A. P., Raabe, I. and Bökel, C. (2012). Hh signalling is essential for
702 somatic stem cell maintenance in the drosophila testis niche. *J Cell Sci* 125, 2663–2669.
703 33. Morrison, S. J. and Spradling, A. C. (2008). Stem Cells and Niches: Mechanisms That
704 Promote Stem Cell Maintenance throughout Life. *Cell* 132, 598–611.
705 34. Nusslein-Volhard, C., Wieschaus, E. and Kluding, H. (1984). Roux's Archives of
706 Developmental Biology Mutations affecting the pattern of the larval cuticle in Drosophila
707 melanogaster I. Zygotic loci on the second chromosome.
708 35. Okegbe, T. C. and di Nardo, S. (2011). The endoderm specifies the mesodermal niche
709 for the germline in Drosophila via Delta-Notch signaling. *Development* 138, 1259–1267.
710 36. Riechmann, V., Rehorn, K.-P., Reuter, R. and Leptin, M. (1998). The genetic control of
711 the distinction between fat body and gonadal mesoderm in Drosophila. *Development*.
712 37. Roach, T. V. and Lenhart, K. F. (2024). Mating-induced Ecdysone in the testis disrupts
713 soma-germline contacts and stem cell cytokinesis. *Development (Cambridge)* 151,.

714 38. Sato, T., Van Es, J. H., Snippert, H. J., Stange, D. E., Vries, R. G., Van Den Born, M.,
715 Barker, N., Shroyer, N. F., Van De Wetering, M. and Clevers, H. (2011). Paneth cells
716 constitute the niche for Lgr5 stem cells in intestinal crypts. *Nature* 469, 415–418.
717 39. Schaub, C., Nagaso, H., Jin, H. and Frasch, M. (2012). Org-1, the Drosophila ortholog of
718 Tbx1, is a direct activator of known identity genes during muscle specification.
719 *Development* 139, 1001–1012.
720 40. Sheng, X. R., Posenau, T., Gumulak-Smith, J. J., Matunis, E., Van Doren, M. and
721 Wawersik, M. (2009). Jak-STAT regulation of male germline stem cell establishment
722 during Drosophila embryogenesis. *Dev Biol* 334, 335–344.
723 41. Sinden, D., Badgett, M., Fry, J., Jones, T., Palmen, R., Sheng, X., Simmons, A.,
724 Matunis, E. and Wawersik, M. (2012). Jak-STAT regulation of cyst stem cell
725 development in the Drosophila testis. *Dev Biol* 372, 5–16.
726 42. Stathopoulos, A., Tam, B., Ronshaugen, M., Frasch, M. and Levine, M. (2004). Pyramus
727 and thisbe: FGF genes that pattern the mesoderm of Drosophila embryos. *Genes Dev*
728 18, 687–699.
729 43. Tanentzapf, G., Devenport, D., Godt, D. and Brown, N. H. (2007). Integrin-dependent
730 anchoring of a stem-cell niche. *Nat Cell Biol* 9, 1413–1418.
731 44. Tseng, C. Y., Burel, M., Cammer, M., Harsh, S., Flaherty, M. S., Baumgartner, S. and
732 Bach, E. A. (2022). chinmo-mutant spermatogonial stem cells cause mitotic drive by
733 evicting non-mutant neighbors from the niche. *Dev Cell* 57, 80-94.e7.
734 45. Tulina, N. and Matunis, E. (2001). Control of Stem Cell Self-Renewal in Drosophila
735 Spermatogenesis by JAK-STAT Signaling. *Science (1979)* 294, 2546–2548.
736 46. Vida, G. S., Botto, E. and Dinardo, S. (2024). *Maintenance of niche architecture requires*
737 *actomyosin and enables proper stem cell signaling and oriented division in the*
738 *Drosophila testis*.
739 47. Walker, M. R., Patel, K. K. and Stappenbeck, T. S. (2009). The stem cell niche. *Journal*
740 *of Pathology* 217, 169–180.
741 48. Warder, B. N., Nelson, K. A., Sui, J., Anllo, L. and DiNardo, S. (2024). An actomyosin
742 network organizes niche morphology and responds to feedback from recruited stem
743 cells.
744 49. Wawersik, M., Milutinovich, A., Casper, A. L., Matunis, E., Williams, B. and Van Doren,
745 M. (2005). Somatic control of germline sexual development is mediated by the
746 JAK/STAT pathway. *Nature* 436, 563–567.

50. Wingert, L. and DiNardo, S. (2015). Traffic jam functions in a branched pathway from Notch activation to niche cell fate. *Development (Cambridge)* 142, 2268–2277.
51. Yamashita, Y., Jones, L. and Fuller, M. (2003). Orientation of Asymmetric StemCell Division by the APC TumorSuppressor and Centrosome. *Science (1979)* 301, 1547–1550.
52. Yamashita, Y. M., Fuller, M. T. and Jones, D. L. (2005). Signaling in stem cell niches: Lessons from the Drosophila germline. *J Cell Sci* 118, 665–672.
53. Zamfirescu, A-M., Yatsenko, AS., and Shcherbata, HR. (2022). Notch signaling sculpts the stem cell niche. Front. Cell Dev. Biol. 10:1027222
54. Zheng, Q., Wang, Y., Vargas, E. and DiNardo, S. (2011). Magu is required for germline stem cell self-renewal through BMP signaling in the Drosophila testis. *Dev Biol* 357, 202–210.

Acknowledgements:

We acknowledge Kirklan Naumuk for technical assistance. We thank Drs. Elizabeth Ables and Beth Thompson, and the Lenhart lab for valuable feedback on the manuscript. We thank the Bloomington *Drosophila* Stock Center (NIH P40OD018537) for stocks, and D. Godt, E. Bach and C. Schaub for antibodies. Work was supported by NIH grants R15 GM154246 to L.A. and R35 GM136270 to S.D.

Author Contributions:

Conceptualization, P.H. and L.A.; methodology, L.A.; validation, P.H. & L.A.; formal analysis, P.H., T.G., and L.A. ; investigation P.H., T.G., and L.A. ; resources S.D. and L.A.; data curation P.H. and L.A.; writing – original draft P.H.; writing – review & editing P.H., S.D., and L.A.; visualization P.H. and L.A.; supervision S.D. and L.A.; project administration S.D. and L.A.; funding acquisition S.D. and L.A.